

Dalton Transactions

Accepted Manuscript



This is an *Accepted Manuscript*, which has been through the Royal Society of Chemistry peer review process and has been accepted for publication.

Accepted Manuscripts are published online shortly after acceptance, before technical editing, formatting and proof reading. Using this free service, authors can make their results available to the community, in citable form, before we publish the edited article. We will replace this *Accepted Manuscript* with the edited and formatted *Advance Article* as soon as it is available.

You can find more information about *Accepted Manuscripts* in the [Information for Authors](#).

Please note that technical editing may introduce minor changes to the text and/or graphics, which may alter content. The journal's standard [Terms & Conditions](#) and the [Ethical guidelines](#) still apply. In no event shall the Royal Society of Chemistry be held responsible for any errors or omissions in this *Accepted Manuscript* or any consequences arising from the use of any information it contains.



www.rsc.org/dalton

**Effect of chalcogens on CO insertion into the palladium-methyl bond of
 $[(N^{\wedge}N^{\wedge}X)Pd(CH_3)]^+$ (X = O, S, Se) and on CO/ethylene copolymerisation**

Kamlesh Kumar and James Darkwa*

Department of Chemistry, University of Johannesburg, Auckland Park Kingsway Campus,
 Auckland Park 2006, South Africa; email: jdarkwa@uj.ac.za

ABSTRACT

Neutral chloromethylpalladium(II) complexes, $[Pd(Cl)(CH_3)(L)]$ (**1a-5a**) with ligands k^2 - $N^{\wedge}S$ -2-((3,5-di-tert-butyl-1H-pyrazol-1-yl)methyl)-6-(phenylthiomethyl)pyridine (**L1**), k^2 - $N^{\wedge}S$ -2-((3,5-dimethyl-1H-pyrazol-1-yl)methyl)-6-(phenylthiomethyl)pyridine (**L2**), k^2 - $N^{\wedge}Se$ -2-((3,5-di-tert-butyl-1H-pyrazol-1-yl)methyl)-6-(phenylselanylmethyl)pyridine (**L3**), k^2 - $N^{\wedge}Se$ -2-((3,5-dimethyl-1H-pyrazol-1-yl)methyl)-6-(phenylselanylmethyl)pyridine (**L4**), k^2 - $N^{\wedge}N$ -2-((3,5-dimethyl-1H-pyrazol-1-yl)methyl)-6-(phenoxyethyl)pyridine (**L5**) have been synthesised and characterised by various spectroscopic techniques. Ligands **L1-L4** exhibit $N_{py}^{\wedge}S/Se$ bidentate coordination whereas **L5** shows $N_{py}^{\wedge}N_{pz}$ bidentate coordination mode in their corresponding neutral palladium complexes. Abstraction of chloride in neutral palladium complexes with $NaBAR_4$ ($BAR_4 =$ tetrakis[3,5-bis(trifluoromethyl)-phenyl]borate) resulted in the formation of the cationic palladium complexes **1b-5b**, in which **L1-L4** adopt a tridentate $N_{pz}^{\wedge}N_{py}^{\wedge}X$ (X = S or Se) coordination mode in their respective cationic palladium complexes (**1b-4b**) whilst **L5** in complex **5b** adopts a $N_{py}^{\wedge}N_{pz}$ bidentate coordination mode and palladium centre is stabilized by the weakly coordinating acetonitrile. Compounds **1b-5b** undergo readily CO insertion into the Pd-CH₃ bond to form Pd-acyl that determine their ability to catalyse CO/ethylene copolymerisation to polyketones.

Introduction

The copolymerisation of nonpolar and polar monomers has received considerable interest in past few decades; in particular the copolymerisation of CO and olefins to produce polyketones.¹⁻⁷ The polyketones obtained from copolymerisation of CO and ethylene possess unique chemical and physical properties (photo- and biodegradability, mechanical strength and chemical resistance), which can be modified to other materials by functionalizing the carbonyl group.⁸ These properties of polyketones can be further modified by changing the comonomers and the catalysts.⁹⁻¹⁴

Late transition metal catalysed CO/ethylene copolymerisation reactions represent a powerful tools for the formation of alternate aliphatic polyketones because of the tolerance of late transition metals for oxygen containing monomers compared to early transition metal counterparts. The most commonly used catalysts are cationic palladium(II) complexes with various bidentate ligands. For example, bidentate phosphine donors (P[^]P),¹⁵⁻²² mixed bidentate phosphorus-oxygen (P[^]O),²³⁻²⁵ mixed bidentate phosphorus-nitrogen (P[^]N)²⁶⁻²⁹ and bidentate nitrogen donors (N[^]N).^{5,30,31} The mechanism of polyketone formation using palladium complexes is well known in the literature and involves the stepwise migratory insertion of CO and ethylene into a palladium-carbon and palladium-acyl bonds respectively.^{3,7,32-39} Vrieze and coworkers in their studies of palladium catalysed copolymerisation of CO and alkenes have established that the rate of CO insertion into the Pd-C bond decreases in the order N-N > P-P > P-N.^{40,41} Although, palladium complexes of diphosphine ligands have widely been used for CO/ethylene copolymerisation, the main problem associated with these complexes is the facile degradation and formation of palladium(0) during the copolymerisation reactions.⁴²⁻⁴⁵ This occurs because of many side reactions such as β -hydride abstraction, reductive elimination and

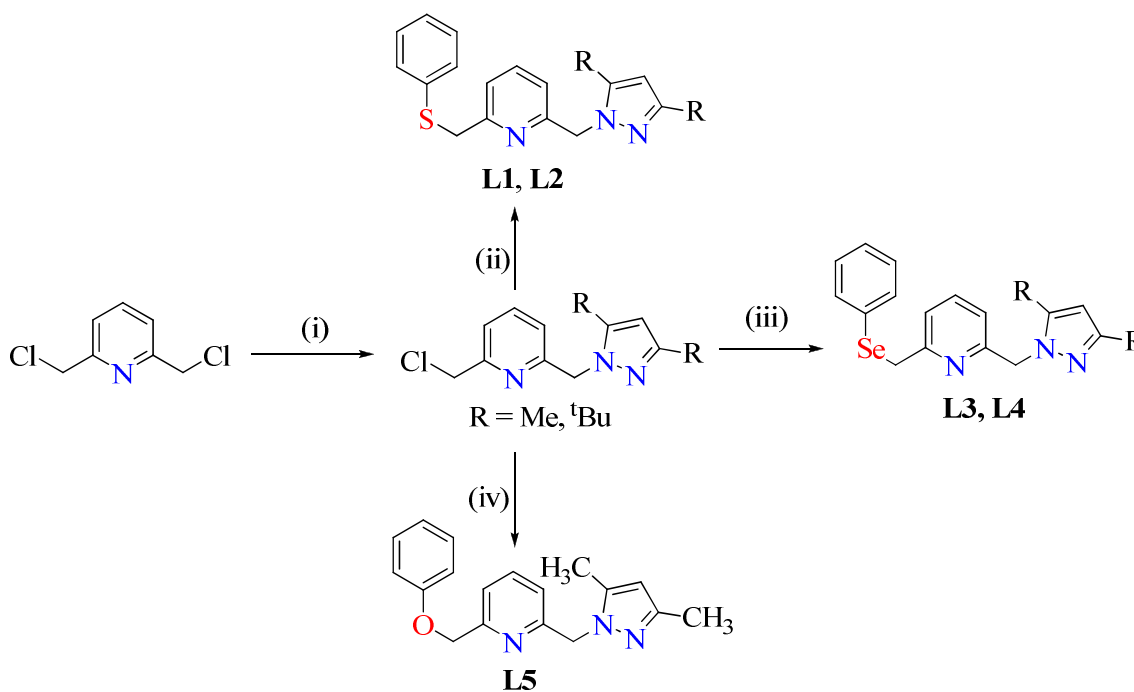
reaction with halogenated solvents. To avoid the deactivation of palladium complex during copolymerisation, Vrieze and coworkers used hemilabile tridentate nitrogen donor ligands and their studies revealed the third nitrogen-donor atom did not sufficiently stabilize the active palladium species but acted as a shuttle for hydrolysis or as an intramolecular base and accelerated the β -hydride elimination reaction.⁴⁶

In a recent study, we reported palladium complexes of tridentate pyrazolyl ligands with pyridinylimine and thienylimine groups that were moderately active catalysts for the copolymerisation of CO/ethylene and CO/styrene.⁴⁷ The moderate activity of our palladium catalysts was attributed to their ability to have one of the nitrogen sites act as a hemilabile group. We, therefore, thought that in making use of this finding of our recent report,⁴⁷ we could introduce chalcogens as the hemilabile donor atoms and modified out the ligand design to a mixed tridentate ligands that have nitrogen and chalcogens (O, S and Se) donor atoms. We thus synthesised $N_{pz}^{\wedge}N_{py}^{\wedge}X$ ($X = O, S$ and Se) tridentate ligands, **L1-L5** (Scheme 1) and used them to prepare neutral (**1a-5a**) and cationic palladium(II) complexes (**1b-5b**) that were investigated as catalysts for the copolymerisation of CO/ethylene. We have also studied CO insertion into Pd-CH₃ bond in all the cationic palladium complexes and this has resulted into their corresponding Pd-acyl complexes. The outcome of this study sheds light on the attempt to use chalcogen atoms as hemilabile donor atoms, which was only partially successful, but offers good insight of how our ligands can be useful in their olefin transformation reactions.

Results and discussion

Syntheses of ligands and complexes

The syntheses of ligands (**L1-L5**) and their neutral chloromethylpalladium(II) complexes (**1a-5a**) are summarized in schemes 1 and 2 respectively. The ligands **L1-L5** were synthesised in good yield from the reaction of alkali metal salt of PhO^- , PhS^- and PhSe^- with 2-(chloromethyl)-6-((3,5-dimethyl-1H-pyrazol-1-yl)methyl)pyridine and 2-(chloromethyl)-6-((3,5-di-tert-butyl-1H-pyrazol-1-yl)methyl)pyridine. Both PhO^- and PhS^- salts were generated from the reactions of phenol or thiophenol with K_2CO_3 and NaOH respectively; but PhSeNa was obtained from the reduction of PhSeSePh with NaBH_4 in ethanol according to the literature procedure.^{48,49} Compounds **L1-L5** are potential $\text{N}_{\text{pz}}^{\wedge}\text{N}_{\text{py}}^{\wedge}\text{X}$ ($\text{X} = \text{O}, \text{S}, \text{Se}$) tridentate ligands that can also bind as either $\text{N}_{\text{py}}^{\wedge}\text{X}$ or $\text{N}_{\text{py}}^{\wedge}\text{N}_{\text{pz}}$ bidentate ligands. Therefore, the substitution reaction of $[\text{Pd}(\text{Cl})(\text{CH}_3)(\text{COD})]$ with these ligands resulted in either the neutral palladium(II) complex as $[\text{Pd}(\text{N}_{\text{py}}^{\wedge}\text{N}_{\text{pz}})(\text{CH}_3)\text{Cl}]$ (type I) or the neutral palladium(II) complexes, $[\text{Pd}(\text{N}_{\text{py}}^{\wedge}\text{X})(\text{CH}_3)\text{Cl}]$ (type II) (Scheme 2).

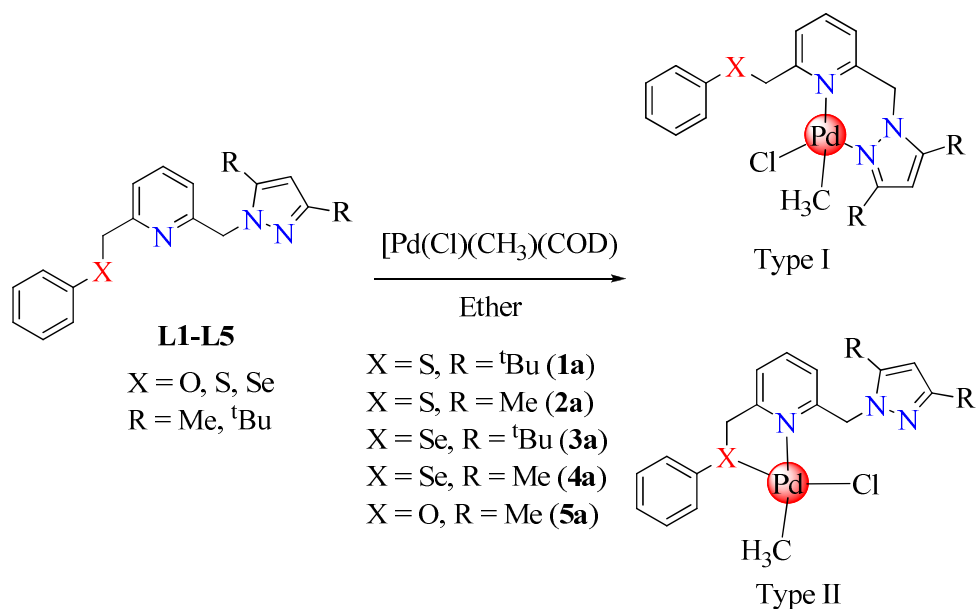


Reagents: (i) Pyrazole, aq. NaOH, aq. TBAH, toluene, 80 °C, 24 h (ii) Thiophenol, NaOH, ethanol, reflux (iii) Diphenyldiselenide, NaBH_4 , ethanol (iv) Phenol, K_2CO_3 , acetonitrile, reflux.

Scheme 1: Synthetic scheme for ligands **L1-L5**

Compounds **L1-L5** and their neutral chloromethylpalladium(II) complexes **1a-5a** were fully characterised by a combination of NMR spectroscopy, high resolution mass spectrometry (HRMS) and in selected cases by single crystal X-ray crystallography. The NMR peaks were consistent with the molecular formulae proposed in Schemes 1 and 2.

Of note in the ^1H NMR spectra of these compounds is the appearance of CH_2 linker peaks, in the ligands which appeared as two sharp singlets (Fig. S1, supporting information), but in the neutral chloromethylpalladium complexes (**1a-5a**) they were unresolved broad singlets at room temperature (Fig. S2, supporting information) which were only resolved at low temperature. A typical variable temperature ^1H NMR spectrum of complex **1a** is shown in Figure 1. At lower temperature, the complex exhibited two different doublets of doublet for both CH_2 linkers. This indicates the rapid molecular motion of the linker protons at room temperature and therefore, these appear protons either as broad singlets or invisible in the room temperature ^1H NMR spectrum. However, the molecular motion considerably slows down at lower temperature and linker CH_2 protons become distereotopic and non-equivalent. Hence, resulting doublets of doublet for each linker CH_2 protons.



Scheme 2: Synthetic scheme for neutral chloromethylpalladium(II) complexes **1a-5a**

The HRMS of complexes **2a** and **4a** showed parent peak at m/z 430.0568 and 478.0018 respectively, assigned to $[M-Cl]^+$ species. However, complexes **1a**, **3a** and **5a** showed various fragments which gave parent peaks that could only be assigned as $[M-Pd-CH_3-Cl \text{ and } H]^+$. None of the five neutral chloromethylpalladium complexes gave molecular ions, but the fragmentation pattern were compatible with the proposed molecular structures.

It is interesting to note that ligands having SPh or SePh group (**L1-L4**) exhibit an $N_{py}^{\wedge}S/Se$ bidentate coordination whereas ligand with OPh group (**L5**) coordinates to palladium centre in an $N_{py}^{\wedge}N_{pz}$ bidentate coordination mode. Confirmation of these coordination modes came from single crystal X-ray structures (for details vide infra). This is not too surprising because sulfur/selenium and palladium are considered soft centres so soft-soft interaction should be favoured in the case of complexes **1a-4a**. However, in complex **5a** the pyrazole nitrogen is

softer than the phenoxy oxygen and therefore the palladium prefers to coordinate with pyrazole nitrogen rather than the oxygen.

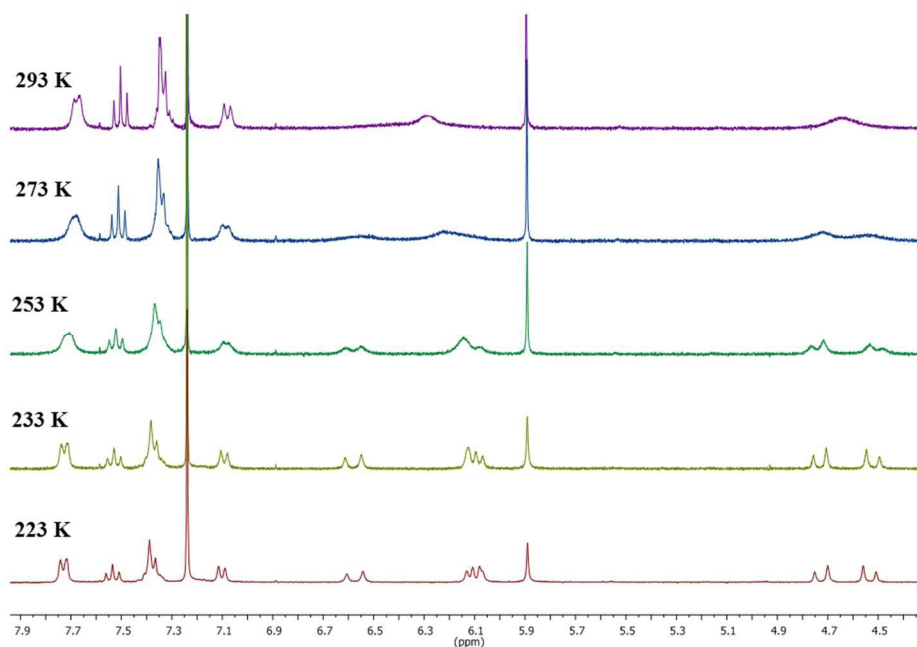
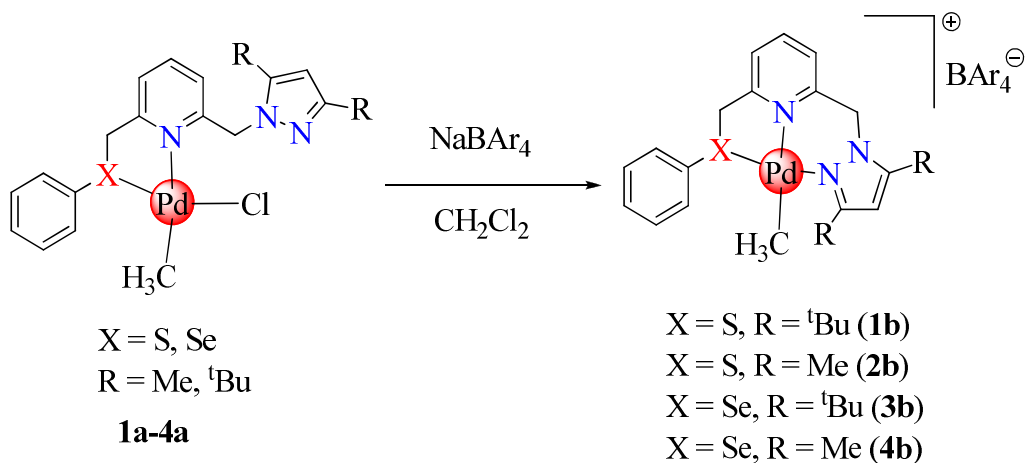
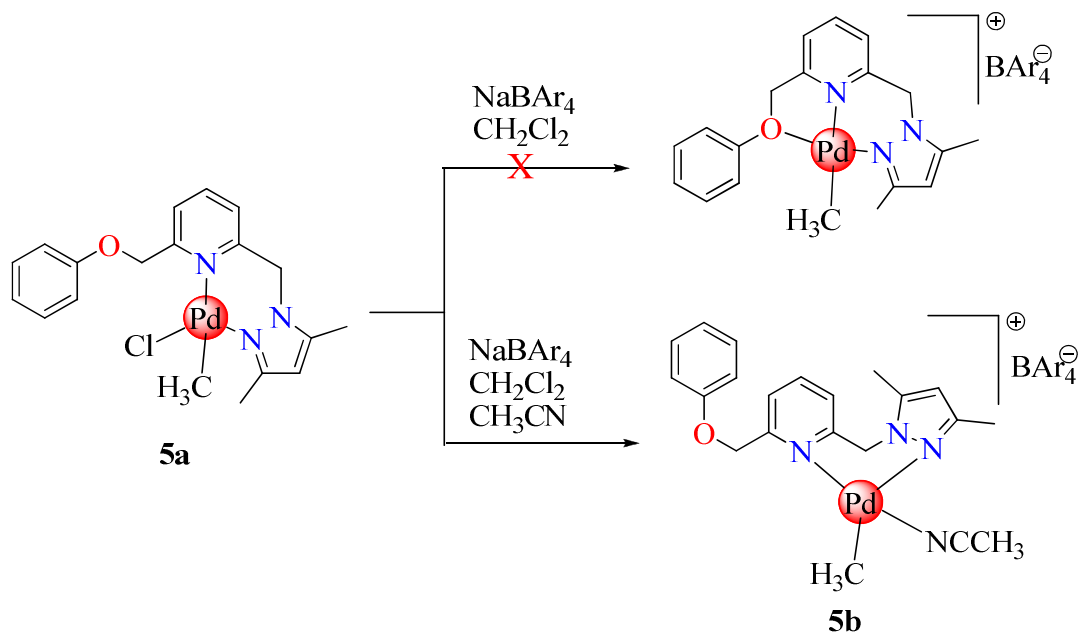


Figure 1: Variable temperature ^1H NMR spectrum for complex **1a**

The cationic methylpalladium(II) complexes, $[\text{Pd}(\text{CH}_3)(\text{L})]\text{BAr}_4$ (**1b-4b**, $\text{L} = \text{L1-L4}$) were synthesised by abstraction of chloride from **1a-4a** using NaBAr_4 ($\text{BAr}_4 = \text{tetrakis}[3,5\text{-bis}(\text{trifluoromethyl})\text{-phenyl]borate}$) in dichloromethane at room temperature (Scheme 3). The vacant coordination site of palladium after abstraction of chloride with NaBAr_4 was occupied by the pyrazole nitrogen and the ligands (**L1-L4**) exhibit $\text{N}_{\text{py}}^{\wedge}\text{N}_{\text{pz}}^{\wedge}\text{X}$ ($\text{X} = \text{S}$ or Se) tridentate coordination mode in the cationic palladium(II) complexes **1b-4b**. Our attempt to synthesise a cationic methylpalladium(II) complex from **5a** under similar reaction conditions resulted in the decomposition of the expected product instantly (Scheme 4), leading to the palladium black. This indicates that after abstraction of chloride from complex **5a** with NaBAr_4 , oxygen atom in

the OPh group is not able to stabilize the palladium centre and this leads to the decomposition and precipitation of palladium black. Therefore, this reaction required a stabilizing agent in the reaction medium and thus subsequent reactions were carried out in a mixture of dichloromethane and acetonitrile; affording the cationic methylpalladium(II) complex, $[\text{Pd}(k^2\text{-N}_{\text{py}}\wedge\text{N}_{\text{pz}})(\text{CH}_3\text{CN})(\text{CH}_3)]\text{BAR}_4$ (**5b**) in a good yield (Scheme 4). The ^1H NMR spectrum of complex **5b** showed a singlet at 1.85 *ppm*, assigned to the methyl of CH_3CN attached to the palladium centre. These revealed that the acetonitrile was able to stabilize the palladium centre in **5b**.

Positive and negative ion mass spectrometry data were collected for complexes **1b-5b** to establish the composition of the cationic palladium(II) complexes. The molecular ions for the cationic species in **2b** and **4b** were obtained at m/z 430.0567 (100%) and m/z 478.0020 (100%) respectively as the parent peaks, whereas molecular ion for **1b** and **3b** were less intense and appeared along with various fragments of the molecule. Complex **5b** did not show molecular ion peak for cationic species but showed other fragments of the molecule. All five palladium salts (**1b-5b**) showed negative ion mass spectral molecular ion peak at m/z 863.0 (100%) confirming the presence of the counter anion $[\text{BAR}_4]^-$ in complexes **1b-5b** and also confirming **1b-5b** as salts made up of cationic palladium species and $[\text{BAR}_4]^-$ anion.

Scheme 3: Synthesis of cationic methylpalladium(II) complexes **1b-4b**Scheme 4: Synthesis of cationic methylpalladium(II) complex **5b**

X-ray crystal structures of neutral chloromethylpalladium(II) complexes **1a** and **5a**

Molecular structures of **1a** and **5a** were determined by single crystal X-ray crystallography. Single crystals suitable for X-ray diffraction analyses were obtained by slow

evaporation of solvents from CH₂Cl₂ solutions of these complexes, kept at -4 °C. The details of crystal data and structure refinement parameters are compiled in Table 1. Molecular structures of **1a** and **5a** with numbering scheme are shown in Figures 2 and 3 respectively. Selected bond lengths and angles for these complexes are given in the figure captions. The palladium metal centre in both complexes displays a distorted square planar coordination geometry as indicated by angles around the palladium centre. The ligands in these complexes exhibited bidentate coordination mode and therefore, four coordination sites of palladium metal centre are occupied by methyl, chloro, pyridine nitrogen (N_{py}) and either sulfur (in complex **1a**) or pyrazole nitrogen (N_{pz}) (in complex **5a**). It is clear from Figures 2 and 3 that the N_{py} and methyl group are trans to each other in both complexes **1a** and **5a**. The Pd-CH₃ bond distances [2.030 (2) and 2.024 (2) Å in **1a** and **5b**, respectively] and Pd-Cl bond distances [2.3393 (5) and 2.3263 (7) Å in **1a** and **5b**, respectively] do not differ too much and also these distances are comparable to Pd-CH₃ and Pd-Cl distances reported in the literature for similar complexes.^{47,50} It is interesting to note the differences in the coordination mode of ligands in both complexes. In complex **1a**, the ligand is coordinated to the palladium metal centre in N_{py}^S bidentate coordination mode, whereas in complex **5a**, the ligand exhibits N_{py}^N_{pz} bidentate coordination mode. These coordination modes can be explained on the basis of soft-soft and hard-hard interactions as discussed earlier.

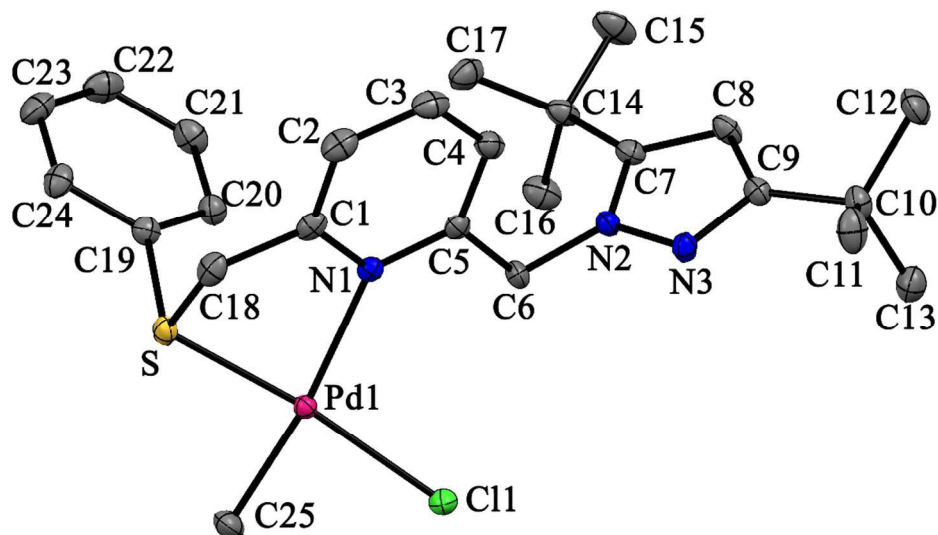


Figure 2: Molecular structure of $[\text{Pd}(k^2\text{-N}_{\text{py}}^{\text{S-L1}})(\text{CH}_3)(\text{Cl})]$ (**1a**) (50% probability ellipsoids). Hydrogen atoms and solvent molecule (CH_2Cl_2) have been omitted for clarity. Selected bond lengths (\AA) and angles ($^\circ$): Pd1-N1 = 2.272 (2); Pd1-S1 = 2.2604 (5); Pd1-Cl1 = 2.3393 (5); Pd1-C25 = 2.030 (2); N1-C1 = 1.357 (2); N1-C5 = 1.352 (2); Cl1-Pd1-C25 = 85.15 (5); Cl1-Pd1-N1 = 102.74 (4); Cl1-Pd1-S1 = 173.30 (2); C25-Pd1-N1 = 171.36 (1); C25-Pd1-S1 = 90.29 (5); S1-Pd1-N1 = 81.54 (4).

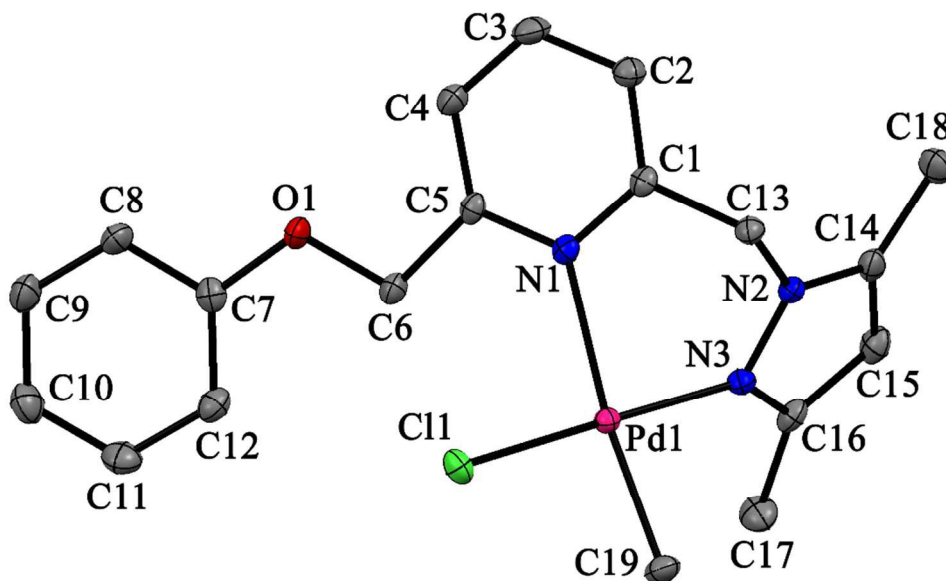


Figure 3: Molecular structure of $[\text{Pd}(k^2\text{-N}_{\text{py}}\text{-N}_{\text{pz}}\text{-L5})(\text{CH}_3)(\text{Cl})]$ (**5a**) (50% probability ellipsoids). Hydrogen atoms and solvent molecule (CH_2Cl_2) have been omitted for clarity. Selected bond lengths (Å) and angles ($^\circ$): Pd1-N1 = 2.228 (1); Pd1-N3 = 2.036 (2); Pd1-C11 = 2.3263 (7); Pd1-C19 = 2.024 (2); N1-C1 = 1.357 (3); N1-C5 = 1.349 (2); C11-Pd1-C19 = 87.39 (6); C11-Pd1-N1 = 96.59 (4); C11-Pd1-N3 = 177.58 (5); C19-Pd1-N1 = 172.56 (7); C19-Pd1-N3 = 91.46 (7); N3-Pd1-N1 = 84.33 (6).

X-ray crystal structures of cationic methylpalladium(II) complexes **1b-4b**.

The molecular structures of the cationic complexes **1b-4b** were also confirmed by X-ray crystallography. Single crystals suitable for X-ray diffraction analyses were similarly obtained from a slow evaporation of solvent from the solution of their respective complexes (methanol/ether for **1b**, CHCl_3 for **3b** and ether for **2b** and **4b**) kept at -4°C . The details of crystal data and structure refinement parameters are compiled in Table 1. It is again clear from Figures 4-7 that all these cationic palladium complexes have similar structure and their palladium centres exhibit distorted square planar coordination geometry. The coordination sites of the palladium are occupied by one ligand and one methyl group. In all complexes, the ligand is coordinated with palladium centre in an $\text{N}_{\text{pz}}\text{-N}_{\text{py}}\text{-X}$ ($\text{X} = \text{S}$ and Se) tridentate coordination fashion and that the pyrazolyl nitrogen occupies the vacant coordination site of palladium created by the abstraction of chloro group. The Pd- N_{py} bond length becomes shorter in the cationic palladium complexes in comparison to the corresponding neutral palladium complex, however the other bond distances (Pd-C and Pd-S) remain essentially the same (compare complexes **1a** and **1b**). We found that the complexes with ditertiary butyl pyrazolyl moiety (**1b** and **3b**) have

longer Pd-N_{pz} and shorter Pd-N_{py} bond distances in comparison to their respective complexes with dimethyl pyrazolyl moiety (**2b** and **4b**). The Pd-C bond length in **3b** is ~0.09 Å longer than complex **4b**. It is not clear if the steric bulk of the tertiary butyl group causes the elongation of the Pd-C bond in **3b**; but definitely influences the size of the N3-Pd-C1 bond angles in **1b** and **3b**.

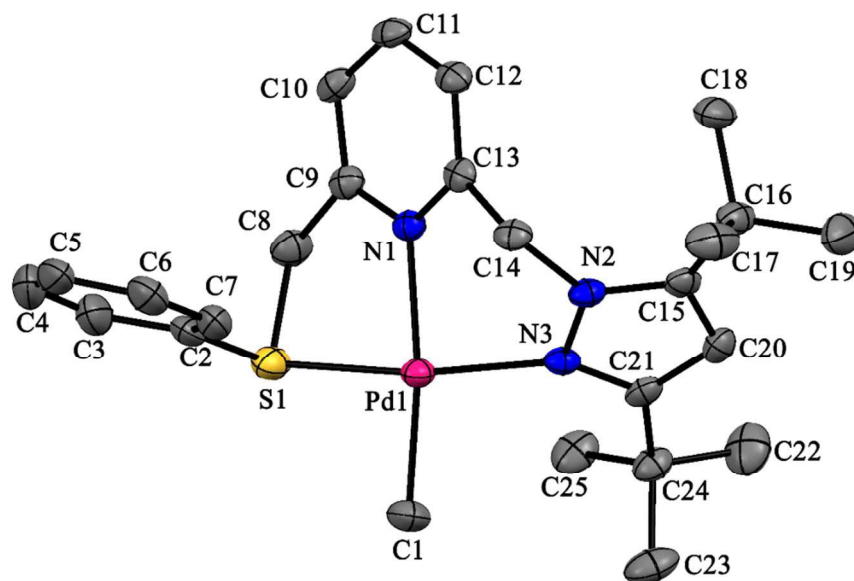


Figure 4: Molecular structure of $[\text{Pd}(k^3\text{-N}_{\text{pz}}\text{-N}_{\text{py}}\text{-S-L1})(\text{CH}_3)]\text{BAR}_4$ (**1b**) (50% probability ellipsoids). Hydrogen atoms and counter anion have been omitted for clarity. Selected bond lengths (Å) and angles (°): Pd1-N1 = 2.105 (2); Pd1-S1 = 2.2723 (8); Pd1-N3 = 2.093 (2); Pd1-C1 = 2.034 (3); N1-C9 = 1.341 (3); N1-C13 = 1.345 (3); N2-N3 = 1.380 (3); S1-Pd1-C1 = 92.64 (8) ; C1-Pd1-N1 = 170.2 (1); C1-Pd1-N3 = 97.1 (1); S1-Pd1-N1 = 83.52 (6); S1-Pd1-N3 = 165.58 (6); N1-Pd1-N3 = 88.49 (8).

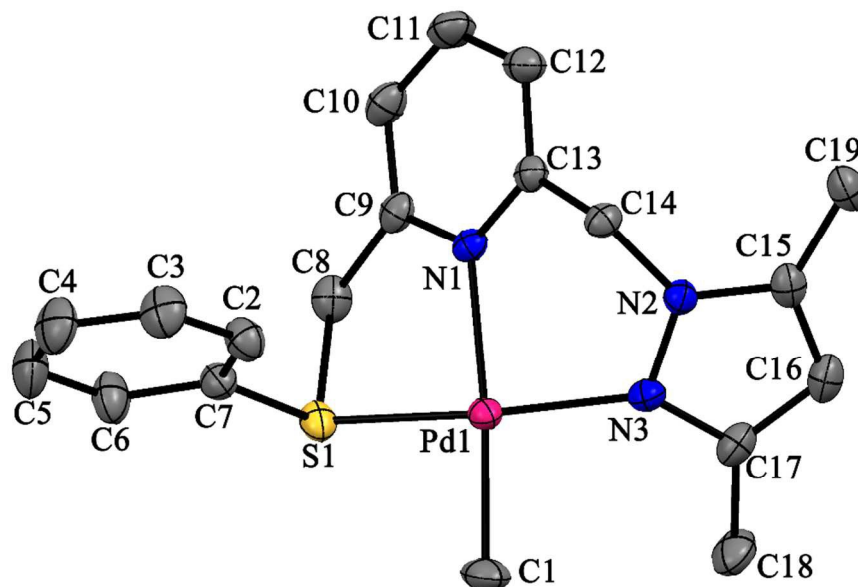


Figure 5: Molecular structure of $[\text{Pd}(k^3\text{-N}_{\text{pz}}\text{N}_{\text{py}}\text{S-L2})(\text{CH}_3)]\text{BAR}_4$ (**2b**) (50% probability ellipsoids). Hydrogen atoms, solvent molecules and counter anion have been omitted for clarity. Selected bond lengths (\AA) and angles ($^\circ$): Pd1-N1 = 2.128 (3); Pd1-S1 = 2.270 (1); Pd1-N3 = 2.068 (3); Pd1-C1 = 2.033 (4); N1-C9 = 1.348 (4); N1-C13 = 1.344 (5); N2-N3 = 1.377 (4); S1-Pd1-C1 = 91.9 (1) ; C1-Pd1-N1 = 174.8 (1); C1-Pd1-N3 = 94.1 (1); S1-Pd1-N1 = 84.26 (8); S1-Pd1-N3 = 167.57 (9); N1-Pd1-N3 = 90.4 (1).

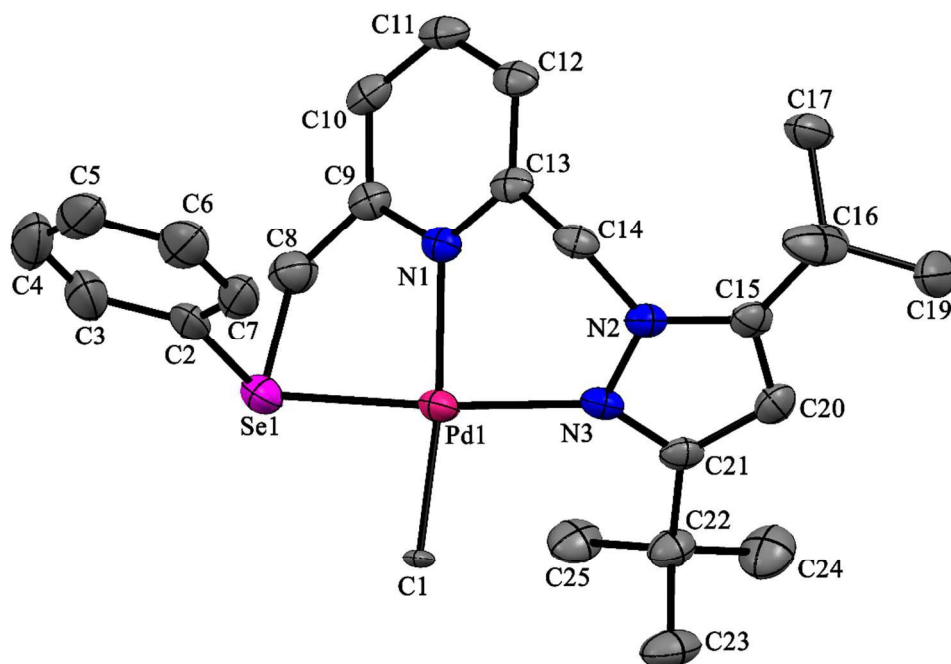


Figure 6: Molecular structure of $[\text{Pd}(k^3\text{-N}_{\text{pz}}^{\wedge}\text{N}_{\text{py}}^{\wedge}\text{Se-L3})(\text{CH}_3)]\text{BAR}_4$ (**3b**) (50% probability ellipsoids). Hydrogen atoms and counter anion have been omitted for clarity. Selected bond lengths (Å) and angles (°): Pd1-N1 = 2.108 (5); Pd1-Se1 = 2.3705 (9); Pd1-N3 = 2.087 (5); Pd1-C1 = 2.105 (5); N1-C9 = 1.347 (7); N1-C13 = 1.336 (7); N2-N3 = 1.389 (6); Se1-Pd1-C1 = 91.8 (1) ; C1-Pd1-N1 = 168.9 (2); C1-Pd1-N3 = 97.1 (2); Se1-Pd1-N1 = 84.4 (1); Se1-Pd1-N3 = 165.5 (1); N1-Pd1-N3 = 88.7 (2).

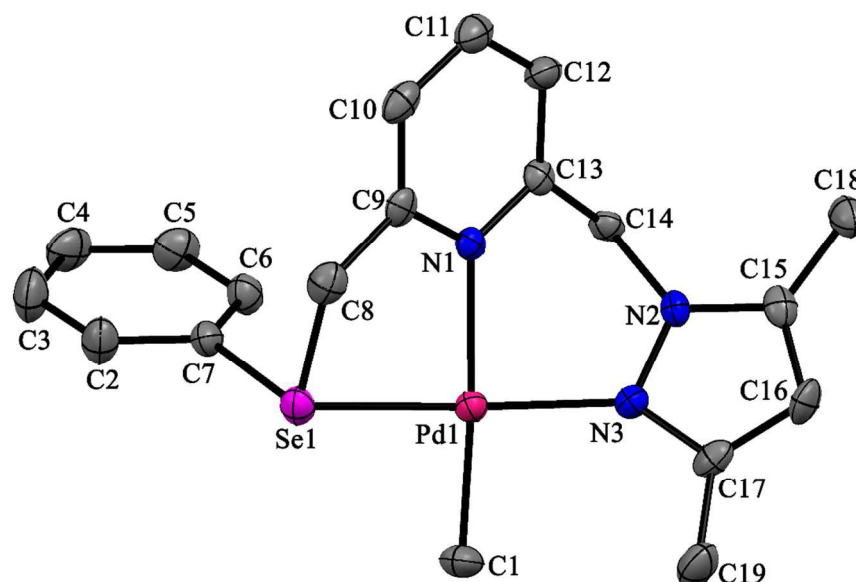


Figure 7: Molecular structure of $[\text{Pd}(k^3\text{-N}_{\text{pz}}^{\text{Npy}}\text{-L4})(\text{CH}_3)]\text{BAR}_4$ (**4b**) (50% probability ellipsoids). Hydrogen atoms, solvent molecules and counter anion have been omitted for clarity. Selected bond lengths (Å) and angles (°): Pd1-N1 = 2.128 (4); Pd1-Se1 = 2.3677 (9); Pd1-N3 = 2.063 (4); Pd1-C1 = 2.027 (5); N1-C9 = 1.347 (6); N1-C13 = 1.349 (6); N2-N3 = 1.377 (5); Se1-Pd1-C1 = 92.1 (2) ; C1-Pd1-N1 = 175.6 (2); C1-Pd1-N3 = 93.0 (2); Se1-Pd1-N1 = 85.2 (1); Se1-Pd1-N3 = 167.2 (1); N1-Pd1-N3 = 90.3 (2).

Carbon monoxide and ethylene copolymerisation reaction

The carbon monoxide and ethylene copolymerisation reaction was investigated using complexes **1a-5a** as catalyst precursors in a solvent mixture of CH_2Cl_2 and Et_2O (1:1 v/v) and in the presence of equimolar amounts of NaBAR_4 . In a typical reaction, a reactor was charged with 0.01 mmol of the complex, in the solvent mixture (5 mL) and then reactor was pressurized with CO (1 MPa) and ethylene (4 MPa). The reaction was stirred at 30 °C for 24 h. However, these

reactions did not result in the formation of polyketone but instead led to the formation of palladium black.

Complex	1a .CH ₂ Cl ₂	5a .CH ₂ Cl ₂	1b	2b .2(C ₄ H ₁₀ O)	3b	4b .2(C ₄ H ₁₀ O)
Empirical formula	C ₂₆ H ₃₆ Cl ₃ N ₃ PdS	C ₃₉ H ₄₆ Cl ₄ N ₆ O ₂ Pd ₂	C ₅₇ H ₄₅ BF ₂₄ N ₃ PdS	C ₅₉ H ₅₄ BF ₂₄ N ₃ O ₂ PdS	C ₅₇ H ₄₆ BF ₂₄ N ₃ PdSe	C ₅₉ H ₅₄ BF ₂₄ N ₃ O ₂ PdSe
Formula weight	635.39	985.42	1377.23	1442.32	1425.14	1489.22
Temperature/K	100(2)	100(2)	100(2)	100(2)	100(2)	100(2)
Crystal system	monoclinic	triclinic	monoclinic	monoclinic	monoclinic	monoclinic
Space group	P2 ₁ /n	P-1	P2 ₁ /c	C2/c	P2 ₁ /c	C2/c
a/Å	12.1170(10)	8.9985(7)	12.9047(10)	41.545(10)	12.922(3)	41.676(3)
b/Å	10.0140(8)	9.7348(8)	21.0538(15)	12.996(3)	21.107(4)	12.9343(10)
c/Å	24.495(2)	12.7904(10)	21.9172(16)	24.090(5)	21.915(5)	24.0868(18)
α/°	90	94.752(2)	90	90	90	90
β/°	103.577(2)	97.174(2)	92.845(2)	104.638(5)	93.167(5)	104.931(2)
γ/°	90	111.388(2)	90	90	90	90
Volume/Å ³	2889.2(4)	1025.05(14)	5947.4(8)	12584(5)	5968(2)	12545.7(17)
Z	4	1	4	8	4	8
ρ _{calc} /cm ³	1.461	1.596	1.538	1.523	1.586	1.577
μ/mm ⁻¹	1.012	1.180	0.463	0.443	1.036	0.991
Crystal size/mm ³	0.496 × 0.259 × 0.115	0.412 × 0.361 × 0.213	0.52 × 0.309 × 0.27	0.64 × 0.372 × 0.24	0.344 × 0.303 × 0.152	0.387 × 0.285 × 0.184
Index ranges	-16 ≤ h ≤ 16 -13 ≤ k ≤ 12 -32 ≤ l ≤ 32	-11 ≤ h ≤ 11 -12 ≤ k ≤ 12 -17 ≤ l ≤ 17	-17 ≤ h ≤ 17 -27 ≤ k ≤ 27 -28 ≤ l ≤ 28	-54 ≤ h ≤ 54 -17 ≤ k ≤ 17 -31 ≤ l ≤ 31	-15 ≤ h ≤ 17 -27 ≤ k ≤ 25 -28 ≤ l ≤ 28	-34 ≤ h ≤ 54 -17 ≤ k ≤ 17 -31 ≤ l ≤ 31
Reflections collected	31520	14648	95309	112608	47324	62804
Data/restraints/parameters	7264/0/314	5045/0/247	14343/12/791	15192/0/827	13654/36/791	15128/0/827
Goodness-of-fit on F ²	1.027	1.038	1.020	1.024	1.039	1.026
Final R indexes [I ≥ 2σ(I)]	R ₁ = 0.0243 wR ₂ = 0.0526	R ₁ = 0.0239 wR ₂ = 0.0521	R ₁ = 0.0419 wR ₂ = 0.1059	R ₁ = 0.0550 wR ₂ = 0.1352	R ₁ = 0.0693 wR ₂ = 0.1679	R ₁ = 0.0618 wR ₂ = 0.1316
Final R indexes [all data]	R ₁ = 0.0294 wR ₂ = 0.0548	R ₁ = 0.0283 wR ₂ = 0.0541	R ₁ = 0.0570 wR ₂ = 0.1161	R ₁ = 0.0772 wR ₂ = 0.1500	R ₁ = 0.1338 wR ₂ = 0.2023	R ₁ = 0.1221 wR ₂ = 0.1591

Table 1: Crystal data and structure refinement parameters for complexes **1a**, **5a** and **1b-4b**

It is well known that CO and olefin insertion reactions occur much easier in complexes with weakly coordinated ligands because of readily available coordination sites for incoming reactants.⁵¹⁻⁵⁴ Therefore, we also synthesised the cationic methylpalladium(II) complexes (**1b-5b**) from their corresponding neutral chloromethylpalladium(II) complexes (**1a-5a**) using NaBAR₄ with assumption that these complexes would have readily available coordination site for CO and ethylene reactions after a hemilabile donor atom leaves the coordination site. The catalytic ability of the cationic palladium complexes (**1b-5b**) for CO and ethylene copolymerization reaction was investigated in dichloromethane. Complexes **1a-4b** were not active catalyst for CO/ethylene copolymerization and thus gave no copolymer in the reactions. However, complex **5b** was found to be moderately active catalyst for this reaction and resulted in a grey coloured precipitate. The precipitate was isolated by filtration, washed with 5 M HCl followed by water and methanol and dried in *vacuo*. The resultant solid was insoluble in all common organic solvents and therefore NMR spectra of the solid material was recorded in hexafluoroisopropanol (HFIP). The NMR data together with FT-IR data was able to identify the solid as a polyketone. The spectroscopic data, GPC and thermal analyses (TGA and DSC) together gave the necessary information of this copolymer.

A typical ¹H NMR spectrum of the polyketone showed a singlet at 2.79 ppm for methylene protons and the ¹³C NMR spectrum showed two peaks at 35.2 and 212.8 ppm assigned for methylene carbon and carbonyl carbon respectively (Fig. S3 and S4, supporting information). This indicated the perfectly alternating nature of polyketone obtained from the above reactions. A typical FT-IR spectrum of the copolymer showed a strong absorption band around ~1690 cm⁻¹ which was assigned to the carbonyl stretching band and a methylene band

(C-H stretching) around $\sim 2910\text{ cm}^{-1}$ (Fig. S5, supporting information). This indicates the presence of $>\text{C}=\text{O}$ and saturated ethylene moieties in the backbone of the polyketone.

The DSC experiments on the copolymers gave a T_g value $\sim 125\text{ }^\circ\text{C}$ and a T_m value $\sim 245\text{ }^\circ\text{C}$ (Fig. S6, supporting information). These T_g and T_m values suggested that the polyketones are crystalline in nature and this is also supported by TGA experiment that showed the polyketone decomposes above $250\text{ }^\circ\text{C}$ (Fig. S7, supporting information). GPC data for selected polyketones showed molecular weight (M_w) of the copolymer in the range of $(1.3\text{-}26.5) \times 10^3$.

We varied the reaction parameters to see their effect on catalytic activity of **5b** in the CO/ethylene copolymerisation. The results are given in Table 2. Although activity of **5b** increases as temperature was increased from 30 to $40\text{ }^\circ\text{C}$ and further increase in temperature resulted in lower activity (Table 2, entries 1-3). All our efforts in increasing CO and ethylene pressure, temperature and time of the copolymerisation reactions did not improve the yield of the polyketones isolated. The highest yield obtained was $\sim 160\text{ mg}$ at 4 MPa ethylene, 1 MPa of CO, $40\text{ }^\circ\text{C}$, and 24 h which gives an activity of $\sim 667\text{ g mol}^{-1}\text{ h}^{-1}$. We suspected that the in situ generated active catalyst containing a Pd-acyl moiety may not be stable and thus we on to investigate the reaction of **5b** with CO which forms the Pd-acyl intermediate.

Table 2: CO and ethylene copolymerisation catalysed by complex **5b**.

Entry	Temp (°C)	Time (h)	Ethylene (MPa)	CO (MPa)	Yield (mg) ^b	Activity (g mol ⁻¹ h ⁻¹)
1	30	24	4	1	110	458
2	40	24	4	1	160	667
3	50	24	4	1	60	250
4	40	3	4	1	57	1900
5	40	10	4	1	78	780
6	40	18	4	1	127	705
7	40	24	3	1	40	167
8	40	24	5	1	153	638
9	40	24	4	2	40	167

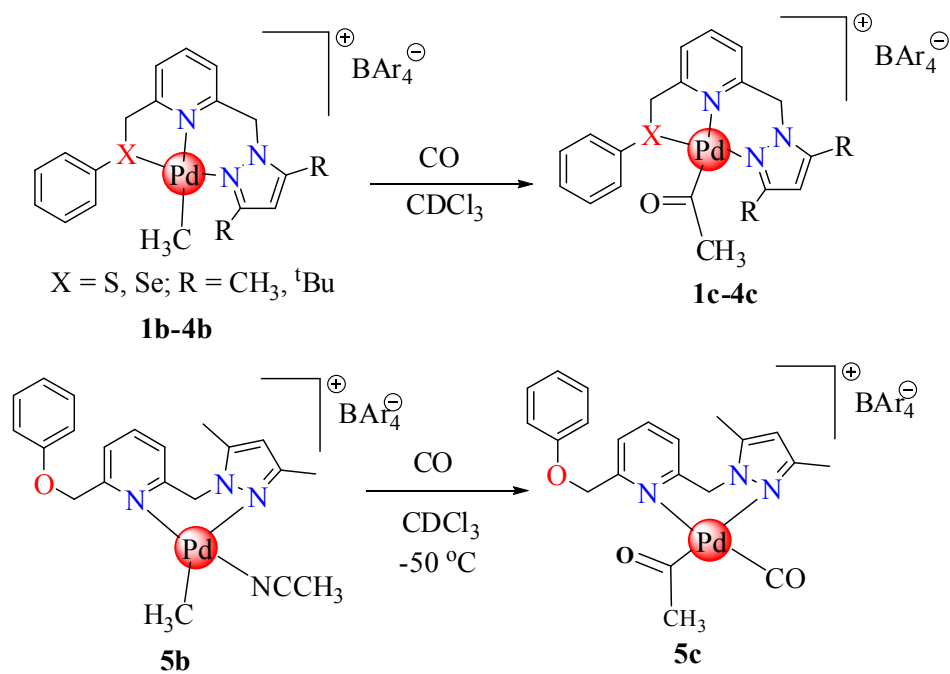
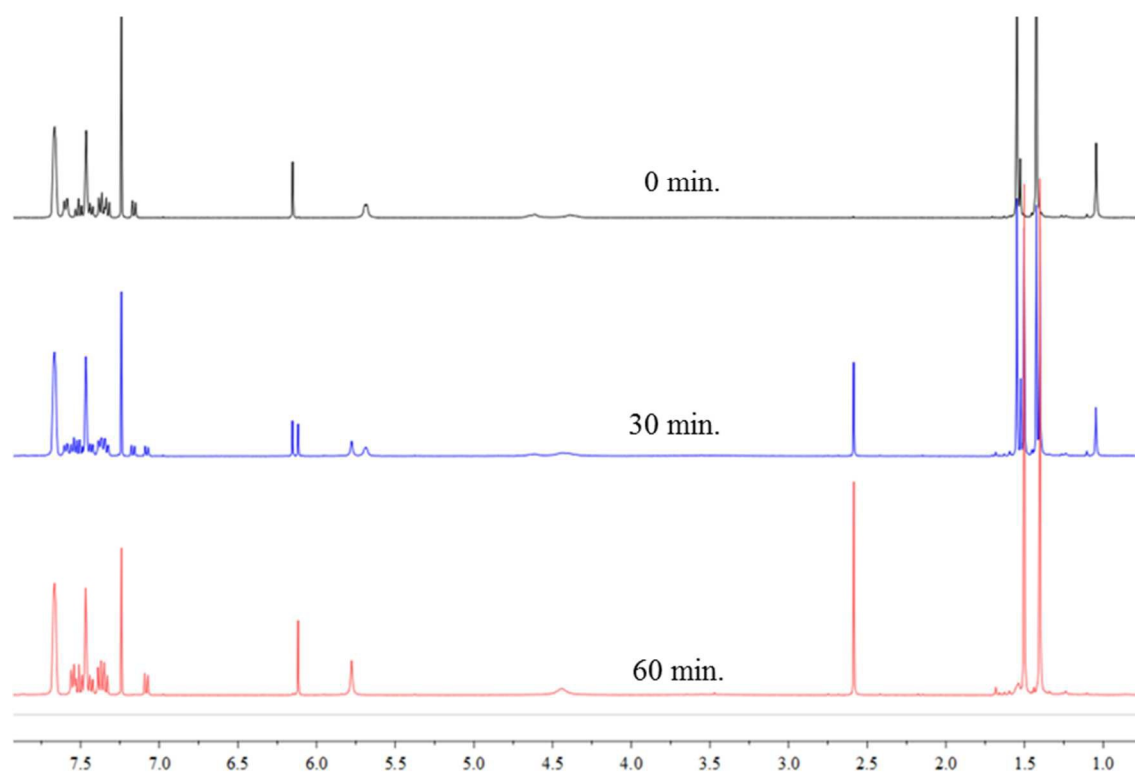
Reaction conditions: Catalyst precursor, 0.01 mmol; CH₂Cl₂, 5.0 mL. ^bYields after purification

Carbon monoxide insertion into palladium-carbon bond in **1b-5b**

Since CO insertion into a Pd-C bond is perceived to be the first step in the CO/ethylene copolymerization reactions, we investigated CO insertion into Pd-CH₃ bonds in the cationic complexes **1b-5b** to find out how facile CO insertion is and also to determine the stability of resultant Pd-acyl intermediate formed after the insertion. In a typical experiment, the solution of respective complex (~7 mg) in CDCl₃ (0.6 mL) in a J. Young NMR tube was evacuated and carefully brought under ~2 atm CO pressure and progress of the reaction was monitored by ¹H NMR spectroscopy at room temperature. Complexes **1b-4b** all undergo facile CO insertion leading to the formation of Pd-acyl products **1c-4c** (Scheme 5) within 1-2 h. The formation of Pd-acyl species was indicated by the disappearance of the methyl singlet of original Pd-CH₃ peak at *ca.* 1.0 ppm and the appearance of the methyl singlet for Pd-C(O)CH₃ singlet peak at *ca.* 2.5-2.6 ppm in the ¹H NMR spectrum. Figure 8 shows the progress of the CO insertion reaction in

the complex **1b**. A similar experiment with complex **5b** under similar conditions used for complexes **1b-4b** was not successful and this was resulted in the formation of palladium black. The CO insertion reaction for **5b** was therefore performed at -50 °C which gave the expected Pd-acyl product **5c** (Scheme 5 and Fig. S8, supporting information). Compound **5c** was decomposed as temperature was raised from -50 °C to 25 °C (Fig. S9, supporting information), but compounds **1c-4c** were quite stable in the solution at room temperature and slowly decomposed when kept for 48 h. It was therefore easy to obtain FT-IR spectra for **1c-4c** which showed $\nu(\text{CO})$ bands around $\sim 1710 \text{ cm}^{-1}$ (Fig. S10, supporting information).

It is clear from the stability of CO inserted products (**1c-5c**) why complexes **1b-4b** were unable to copolymerise CO and ethylene but complex **5b** could. In **1c-4c** the coordination of pyrazole nitrogen to the palladium centre makes it difficult for the next reactions in the copolymerisation, which involve ethylene coordination and insertion. This is difficult if not impossible because the Pd-N_{pz} bond is stronger than the Pd-|| expected bond. A DFT calculation to establish ethylene coordination barrier for $[\text{Pd}(\text{k}^3\text{-N}^{\wedge}\text{N}^{\wedge}\text{N})(\text{CH}_3)]^+$ (N[^]N[^]N = 2,6-bis(pyrazolyl)pyridine) shows the ethylene coordination is thermodynamically unfavourable ($\Delta H = +1.7 \text{ kcal/mol}$; $\Delta G = +12.6 \text{ kcal/mol}$).⁵⁵ This implies that the activity of **5b** is via the formation of active species which has a hemilabile phenoxy group that allows ethylene coordination for the copolymerisation to occur. The moderate activity of **5b**, however suggest that this hemilabile behaviour of phenoxy group is not very stable; hence the observation of palladium black as a sign of catalyst decomposition.

Scheme 5: CO insertion reaction in the complexes **1b-5b**Figure 8: Insertion of CO in Pd-CH₃ bond in complex **1b** monitored by ¹H NMR

Conclusions

In this study, we have prepared a series of neutral and cationic palladium(II) complexes of $N_{pz}^{\wedge}N_{py}^{\wedge}X$ ($X = O, S,$ and Se) tridentate ligands with soft and hard donors sites. These potentially tridentate ligands exhibit bidentate coordination modes in their neutral palladium complexes. However, the denticity of the ligands in the cationic palladium complexes depends on the nature of the chalcogen in the ligand. We have also demonstrated that CO insertion reaction into Pd-CH₃ bond in all the cationic palladium complexes is facile and forms their corresponding Pd-acyl complexes. The four cationic palladium complexes that have sulfur and selenium in their ligands do not catalyse CO/ethylene copolymerisation because these are unable to activate ethylene. However, the cationic palladium complex which has the more hemilabile phenoxy group activates the ethylene to form polyketones; albeit with moderate activity because of catalyst decomposition.

Experimental section

Material and general methods

Unless otherwise stated, all manipulations were carried out under nitrogen or argon atmosphere using standard Schlenk techniques. All organic solvents were dried and purified by distillation over standard reagents under argon prior to use. The reagents used in this study, 2,6-pyridinedimethanol, 3,5-dimethylpyrazole, 2,2,6,6-tetramethyl-3,5-heptadione, phenol, thiophenol, diphenyldiselenide, tetrabutylammonium hydroxide (TBAH) and hexafluoroisopropanol (caution! HFIP is highly toxic) were purchased from Sigma-Aldrich while NaBAR₄ (BAR₄ = tetrakis[3,5-bis(trifluoromethyl)-phenyl]borate) was purchased from Alfa-Aesar

and used as received without further purification. The starting materials, 2,6-bis(chloromethyl)pyridine,⁵⁶ 3,5-di-*tert*-butylpyrazole,⁵⁷ [Pd(Cl)(CH₃)(COD)],⁵⁸ 2-(chloromethyl)-6-((3,5-dimethyl-1H-pyrazol-1-yl)methyl)pyridine⁵⁹ and 2-(chloromethyl)-6-((3,5-di-*tert*-butyl-1H-pyrazol-1-yl)methyl)pyridine⁵⁹ were synthesised according to literature procedures.

Fourier transform-Infrared (FT-IR) spectra were recorded on a Bruker Tensor 27 equipped with a Diamond ATR. Elemental analyses were performed on a Thermo Scientific Flash 2000 Elemental analyzer. NMR spectra were recorded on a Bruker 400 MHz instrument (¹H at 400 MHz and ¹³C at 100 MHz). The chemical shift values (δ) are reported in *ppm* and referenced to the residual proton and carbon signals at 7.24 and 77.0 *ppm*, respectively of CDCl₃ NMR solvent. HRMS spectra were recorded on a Waters Synapt G2 instrument. Differential scanning calorimetry (DSC) measurements were performed on a Mettler Toledo DSC 822e instrument at a heating and cooling rate of 10 °C min⁻¹, and the reported T_g values were determined during the heating process. Thermogravimetric analyses (TGA) were performed on a SDT Q600 TA instrument at a heating rate of 10 °C min⁻¹.

X-ray structure determination

Single crystal X-ray diffraction data were collected on a Bruker APEXII diffractometer with Mo K α ($\lambda = 0.71073$ Å) radiation and a detector to crystal distance of 4.00 cm. The initial cell matrix was obtained from three series of scans at different starting angles. Each series consisted of 12 frames collected at intervals of 0.5° in a 6° range with an exposure time of about 10 s per frame. The reflections were successfully indexed by an automated indexing routine built in the APEXII program suite. The data were collected using the full sphere data collection routine to survey the reciprocal space to the extent of a full sphere to a resolution of 0.75 Å. Data

were harvested by collecting 2982 frames at intervals of 0.5° scans in ω and ϕ with exposure times of 10 s per frame.⁶⁰ The data integration and reduction were processed with SAINT software. A multi-scan absorption correction was applied to the collected reflections with SADABS using XPREP. Structures were solved by the direct method using the program SHELXS-97 and were refined on F^2 by the full-matrix least-squares technique using the SHELXL-97 program package. All non-hydrogen atoms were refined with anisotropic displacement coefficients. All hydrogen atoms were included in the structure factor calculations at idealized positions and were allowed to ride on the neighboring atoms with relative isotropic displacement coefficients.⁶¹

Synthesis of 2-((3,5-di-tert-butyl pyrazol-1-yl)methyl)-6-(phenylthiomethyl)pyridine (L1)

An aqueous solution of NaOH (100 mg, 2.5 mmol) in 3 mL water was added to the solution of thiophenol (220.4 mg, 2.0 mmol) in 30 mL ethanol. The reaction mixture was refluxed for 1 h and a solution of 2-(chloromethyl)-6-((3,5-di-tert-butyl-1H-pyrazol-1-yl)methyl)pyridine (638.4 mg, 2.0 mmol) in 15 mL ethanol was added dropwise to the reaction. The reaction mixture was further refluxed for 5 h. After completion of the reaction, solvent was evaporated on rotary evaporator. The residue obtained was dissolved in dichloromethane (30 mL) and washed with water (3 x 10 mL). The dichloromethane layer was separated and dried over anhydrous MgSO_4 . The evaporation of solvent on rotary evaporator gave pure white solid product. Yield: 708.4 mg (~90%). ^1H NMR (400 MHz, CDCl_3 , δ ppm): 7.43 (t, 1H, $J = 7.6$ Hz), 7.28 (d, 2H, $J = 8.0$ Hz), 7.21 (t, 2H, $J = 7.4$ Hz), 7.16-7.11 (m, 2H), 6.28 (d, 1H, $J = 7.6$ Hz), 5.91 (s, 1H), 5.53 (s, 2H), 4.21 (s, 2H), 1.30 (s, 9H), 1.20 (s, 9H). $^{13}\text{C}\{^1\text{H}\}$ NMR (100 MHz, CDCl_3 , δ ppm): 160.74, 159.08, 156.7, 152.02, 137.42, 135.64, 129.66, 128.79, 126.28, 121.08,

119.05, 100.46, 56.28, 40.29, 31.93, 31.28, 30.60, 30.19. HRMS (ESI): m/z (%) 394.2314 ($[M+H]^+$, 100%).

Synthesis of 2-((3,5-dimethyl-1H-pyrazol-1-yl)methyl)-6-(phenylthiomethyl)pyridine (L2)

This was synthesised following the procedure used for the synthesis of ligand L1 using NaOH (72 mg, 1.8 mmol), 2-(chloromethyl)-6-((3,5-dimethyl-1H-pyrazol-1-yl)methyl)pyridine (353.6 mg, 1.5 mmol) and thiophenol (165.3 mg, 1.5 mmol). The product was obtained as light yellow liquid. Yield: 401 mg (~86%). ^1H NMR (400 MHz, CDCl_3 , δ ppm): 7.48 (t, 1H, $J = 7.6$ Hz), 7.29 (d, 2H, $J = 7.6$ Hz), 7.21 (t, 2H, $J = 7.6$ Hz), 7.18-7.13 (m, 2H), 6.56 (d, 1H, $J = 7.6$ Hz), 5.85 (s, 1H), 5.28 (s, 2H), 4.21 (s, 2H), 2.23 (s, 3H), 2.13 (s, 3H). $^{13}\text{C}\{^1\text{H}\}$ NMR (100 MHz, CDCl_3 , δ ppm): 157.15, 157.01, 147.91, 139.65, 137.59, 135.56, 129.55, 128.73, 126.25, 121.49, 118.99, 105.59, 54.21, 40.21, 13.46, 10.99. HRMS (ESI): m/z (%) 310.1379 ($[M+H]^+$, 100%).

Synthesis of 2-((3,5-di-tert-butyl-1H-pyrazol-1-yl)methyl)-6-(phenylselanylmethyl)pyridine (L3)

A solution of NaBH_4 (37.8 mg, 1.0 mmol) in 2 mL of 5% aqueous NaOH was added to the solution of diphenyldiselenide (156.1 mg, 0.5 mmol) in ethanol (15 mL) under argon. The solution became colorless after addition of NaBH_4 solution indicating the formation of sodium phenylselenolate (PhSeNa). Now a solution of 2-(chloromethyl)-6-((3,5-di-tert-butyl-1H-pyrazol-1-yl)methyl)pyridine (319.2 mg, 1.0 mmol) in 10 mL ethanol was added dropwise to the reaction mixture and stirred further for 5 h at room temperature. After completion of the reaction,

solvent was evaporated on rotary evaporator. The residue obtained was dissolved in dichloromethane (20 mL) and washed with water (3 x 7 mL). The organic layer was collected and dried over anhydrous MgSO₄. After removal of solvent on rotary evaporator a light yellow solid product was obtained. Yield: 412.8 mg (~94%). ¹H NMR (400 MHz, CDCl₃, δ ppm): 7.45 (d, 1H, J = 1.6 Hz), 7.43(d, 1H, J = 2.4 Hz), 7.37 (t, 1H, J = 7.6 Hz), 7.22-7.18 (m, 3H), 6.88 (d, 1H, J = 7.6 Hz), 6.23 (d, 1H, J = 8.0 Hz), 5.91 (s, 1H), 5.50 (s, 2H), 4.17 (s, 2H), 1.30 (s, 9H), 1.21 (s, 9H). ¹³C{¹H} NMR (100 MHz, CDCl₃, δ ppm): 160.67, 159.10, 157.67, 151.98, 137.16, 133.67, 129.69, 128.91, 127.35, 121.13, 118.66, 100.04, 56.24, 33.57, 31.91, 31.25, 30.58, 30.17. HRMS (ESI): m/z (%) 442.1763 ([M+H]⁺, 100%).

Synthesis of 2-((3,5-dimethyl-1H-pyrazol-1-yl)methyl)-6-(phenylselanylmethyl)pyridine (L4)

This ligand was synthesised following the procedure used for the synthesis of ligand **L3** using NaBH₄ (56.7 mg, 1.5 mmol), diphenyldiselenide (234.0 mg, 0.75 mmol) and 2-(chloromethyl)-6-((3,5-dimethyl-1H-pyrazol-1-yl)methyl)pyridine (353.5 mg, 1.5 mmol). The product was obtained as light yellow liquid. Yield: 451.1 mg (~84%). ¹H NMR (400 MHz, CDCl₃, δ ppm): 7.45-7.41 (m, 3H), 7.23-7.18 (m, 3H), 6.97 (d, 1H, J = 7.6 Hz), 6.51 (d, 1H, J = 7.6 Hz), 5.85 (s, 1H), 5.25 (s, 2H), 4.18 (s, 2H), 2.23 (s, 3H), 2.13 (s, 3H). ¹³C{¹H} NMR (100 MHz, CDCl₃, δ ppm): 158.22, 157.06, 147.86, 139.64, 137.35, 133.57, 129.70, 128.87, 127.30, 121.53, 118.63, 105.58, 54.26, 33.48, 13.46, 11.01. HRMS (ESI): m/z (%) 358.0818 ([M+H]⁺, 100%).

Synthesis of 2-((3,5-dimethyl-1H-pyrazol-1-yl)methyl)-6-(phenoxyethyl)pyridine (L5)

A mixture of 2-(chloromethyl)-6-((3,5-dimethyl-1H-pyrazol-1-yl)methyl)pyridine (235.7 mg, 1.0 mmol), phenol (141 mg, 1.5 mmol), and K_2CO_3 (415 mg, 3.0 mmol) in acetonitrile (20 mL) was heated under reflux for 24 h. After cooling to the room temperature, reaction mixture was filtered and residue was washed with acetonitrile (2 x 3 mL). The solvent was evaporated from combined acetonitrile fraction under reduced pressure. The resulting compound was dissolved in dichloromethane (20 mL) and washed with 2% aq. NaOH (2 x 10 mL) followed by water to remove excess phenol. The dichloromethane fraction was collected and dried over anhydrous $MgSO_4$. The removal of dichloromethane was resulted pure titled compound as brown liquid. Yield: 270 mg (~92%). 1H NMR (400 MHz, $CDCl_3$, δ ppm): 7.58 (t, 1H, J = 8.0 Hz), 7.38 (d, 1H, J = 8.0 Hz), 7.27 (t, 3H, J = 8.0 Hz), 6.96 (d, 2H, J = 7.6 Hz), 6.64 (d, 1H, J = 7.6 Hz), 5.87 (s, 1H), 5.33 (s, 2H), 5.16 (s, 2H), 2.24 (s, 3H), 2.17 (s, 3H). $^{13}C\{^1H\}$ NMR (100 MHz, $CDCl_3$, δ ppm): 158.28, 157.02, 156.90, 148.08, 139.69, 137.84, 129.49, 121.11, 119.81, 119.59, 114.75, 105.68, 70.38, 54.27, 13.52, 11.06. HRMS (ESI): m/z (%) 294.1603 ($[M+H]^+$, 100%).

Synthesis of $k^2-N_{py}^S-2-((3,5-di-tert-butyl-1H-pyrazol-1-yl)methyl)-6-(phenylthiomethyl)pyridinechloromethylpalladium(II)$ (1a).

A solution of ligand **L1** (393.6 mg, 1.0 mmol) in dry ether (20 mL) was added dropwise to the suspension of $[Pd(Cl)(CH_3)(COD)]$ (265.1 mg, 1.0 mmol) in dry ether (20 mL) under argon. A clear solution was obtained after the addition of ligand and in few minutes white product was started precipitating. The reaction mixture was further stirred for 24 h at room temperature under argon. The off white solid product was filtered and washed with ether (2 x 5 mL) and dried under vacuum. Yield: 430 mg (~78%). 1H NMR (400 MHz, $CDCl_3$, δ ppm): 7.68

(d, 2H, $J = 5.6$ Hz), 7.50 (t, 1H, $J = 7.6$ Hz), 7.34-7.33 (m, 3H), 7.08 (d, 1H, $J = 6.8$ Hz), 6.48 (bs, 1H), 6.27 (bs, 2H), 5.89 (s, 1H), 4.68 (bs, 2H), 1.29 (s, 18H), 1.13 (s, 3H). Elemental analysis (%) calcd. For $C_{25}H_{34}ClN_3PdS$: C, 54.54; H, 6.23; N, 7.63. Found: C, 54.31; H, 6.23; N, 7.47. HRMS (ESI): m/z 514.1511 ($[M-Cl]^+$, 5%), 394.2342 $[M-Pd-CH_3-Cl+H]^+$, 100%.

Synthesis of $k^2-N_{py}^{\wedge}S-2-((3,5\text{-dimethyl-1H-pyrazol-1-yl)methyl)-6-(phenylthiomethyl)pyridinechloromethylpalladium(II)$ (2a).

Complex **2a** was synthesised from ligand **L2** (309.4 mg, 1.0 mmol) and $[Pd(Cl)(CH_3)(COD)]$ (265.1 mg, 1.0 mmol) according to the procedure used for the synthesis of complex **1a**. Yield: 405.5 mg (~87%). 1H NMR (400 MHz, $CDCl_3$, δ ppm): 7.70 (m, 2 H), 7.44 (d, 1H, $J = 7.2$ Hz), 7.35 (s, 2H), 7.20-7.18 (m, 3H), 5.92 (s, 3H), 4.91 (s, 2H), 2.42 (s, 3H), 2.36 (s, 3H), 1.00 (s, 3H). Elemental analysis (%) calcd. For $C_{19}H_{22}ClN_3PdS$: C, 48.94; H, 4.76; N, 9.01. Found: C, 48.82; H, 4.74; N, 8.87. HRMS (ESI): m/z 430.0568 ($[M-Cl]^+$, 100%).

Synthesis of $k^2-N_{py}^{\wedge}Se-2-((3,5\text{-di-tert-butyl-1H-pyrazol-1-yl)methyl)-6-(phenylselanylmethyl)pyridinechloromethylpalladium(II)$ (3a).

Complex **3a** was synthesised from ligand **L3** (362.7 mg, 0.82 mmol) and $[Pd(Cl)(CH_3)(COD)]$ (218.3 mg, 0.82 mmol) according to the procedure used for the synthesis of complex **1a**. Yield: 450.1 mg (~75%). 1H NMR (400 MHz, $CDCl_3$, δ ppm): 7.72 (d, 2H, $J = 7.6$ Hz), 7.46 (t, 1H, 7.6 Hz), 7.38-7.28 (m, 3H), 7.04 (d, 1H, $J = 7.6$ Hz), 6.40 (s, 2H), 6.26 (d, 1H, $J = 6.0$ Hz), 5.89 (s, 1H), 4.68 (s, 2H), 1.33 (s, 9H), 1.30 (s, 9H), 1.03 (s, 3H). Elemental analysis (%) calcd. For $C_{25}H_{34}ClN_3PdSe \cdot 0.5CH_2Cl_2$: C, 47.87; H, 5.51; N, 6.57. Found: C, 47.87; H, 5.72; N, 6.34. HRMS (ESI): m/z 514.1511 ($[M-Cl]^+$, 5%), 442.1760 $[M-Pd-CH_3-Cl+H]^+$, 100%.

Synthesis of k^2 -N_{py}[^]Se-2-((3,5-dimethyl-1H-pyrazol-1-yl)methyl)-6-(phenylselanylmethyl)pyridinechloromethylpalladium(II) (4a).

Complex **4a** was synthesised from ligand **L4** (178.2 mg, 0.5 mmol) and [Pd(Cl)(CH₃)(COD)] (132.5 mg, 0.5 mmol) according to the procedure used for the synthesis of complex **1a**. Yield: 210 mg (~82%). ¹H NMR (400 MHz, CDCl₃, δ ppm): 7.77 (d, 1H, J = 5.2 Hz), 7.64 (t, 1H, J = 7.6 Hz), 7.45 (d, 2H, J = 7.2 Hz), 7.27 (t, 2H, J = 7.2 Hz), 7.22-7.18 (m, 2H), 5.93 (s, 1H), 5.89 (bs, 2H), 4.85 (bs, 2H), 2.47 (s, 3H), 2.37 (s, 3H), 0.99 (s, 3H). Elemental analysis (%) calcd. For C₁₉H₂₂ClN₃PdSe: C, 44.46; H, 4.32; N, 8.19. Found: C, 44.87; H, 4.54; N, 8.28. HRMS (ESI): m/z 478.0018 ([M-Cl]⁺, 100%).

Synthesis of k^2 -N_{py}[^]N_{pz}-2-((3,5-dimethyl-1H-pyrazol-1-yl)methyl)-6-(phenoxymethyl)pyridinechloromethylpalladium(II) (5a).

Complex **5a** was synthesised from ligand **L5** (293.4 mg, 1.0 mmol) and [Pd(Cl)(CH₃)(COD)] (265.1 mg, 1.0 mmol) according to the procedure used for the synthesis of complex **1a**. Yield: 361.2 mg (~80%). ¹H NMR (400 MHz, CDCl₃, δ ppm): 7.73 (t, 1H, J = 7.6 Hz), 7.67 (d, 1H, J = 7.6 Hz), 7.28-7.21 (m, 4H), 7.06 (d, 2H, J = 8.0 Hz), 6.94 (t, 1H, J = 7.2 Hz), 6.62 (d, 1H, J = 14.8), 6.10 (d, 1H, J = 15.2 Hz), 5.88 (s, 1H), 5.71 (d, 1H, J = 15.2 Hz), 5.13 (d, 1H, J = 14.8 Hz), 2.32 (d, 6H, J = 2.8 Hz), 1.05 (s, 3H). Elemental analysis (%) calcd. For C₁₉H₂₂ClN₃PdO: C, 50.68; H, 4.92; N, 9.33. Found: C, 50.61; H, 4.89; N, 9.25. HRMS (ESI): m/z 414.0795 ([M-Cl]⁺, 10%), 294.1599 [M-Pd-CH₃-Cl and H]⁺, 100%).

Synthesis of k^3 -N_{pz}[^]N_{py}[^]S-2-((3,5-di-tert-butyl-1H-pyrazol-1-yl)methyl)-6-(phenylthiomethyl)pyridinemethylpalladium(II) tetrakis(3,5-trifluoromethylphenyl)borate (1b).

A mixture of complex **1a** (110.1 mg, 0.2 mmol) and NaBAR₄ (177.2 mg, 0.2 mmol) in dichloromethane (20 mL) was stirred at room temperature for 3 h under argon. The reaction mixture was filtered through small pad of Celite and solvent was evaporated in *vacuo* to obtain foaming light yellow solid product. Yield: 255 mg (~92%). ¹H NMR (400 MHz, CDCl₃, δ ppm): 7.67 (s, 8H), 7.59 (d, 2H, J = 7.6 Hz), 7.53 (t, 1H, J = 7.6 Hz), 7.47 (s, 4H), 7.42 (d, 1H, J = 7.2 Hz), 7.38-7.32 (m, 3H), 7.17 (d, 1H, J = 7.6 Hz), 6.15 (s, 1H), 5.69 (d, 2H, J = 6.0 Hz), 4.62 (bs, 1H), 4.39 (bs, 1H), 1.55 (s, 9H), 1.42 (s, 9H), 1.04 (s, 3H). Elemental analysis (%) calcd. For [C₂₅H₃₄N₃PdS]⁺[BAR₄]⁻: C, 49.67; H, 3.36; N, 3.05. Found: C, 49.26; H, 3.35; N, 2.76. Positive ion ESI-MS: m/z (%) = 514.1509 (10%) [M]⁺. Negative ion ESI-MS: m/z (%) 863.0659 (100%) [M]⁻.

Synthesis of k^3 -N_{pz}[^]N_{py}[^]S-2-((3,5-dimethyl-1H-pyrazol-1-yl)methyl)-6-(phenylthiomethyl)pyridinemethylpalladium(II) tetrakis(3,5-trifluoromethylphenyl)borate (2b).

Complex **2b** was synthesised from complex **2a** (100 mg, 0.214 mmol) and NaBAR₄ (189.6 mg, 0.214 mmol) according to procedure used for the synthesis of complex **1b**. Yield: 181 mg (~65%). ¹H NMR (400 MHz, CDCl₃, δ ppm): 7.67 (s, 8H), 7.64 (d, 2H, J = 8.0 Hz), 7.52 (t, 1H, J = 8.0 Hz), 7.46 (s, 4H), 7.44 (d, 1H, J = 7.6 Hz), 7.38 (t, 2H, J = 7.6 Hz), 7.22 (t, 2H, J = 7.6 Hz), 6.01 (s, 1H), 5.25 (s, 2H), 4.52 (bs, 2H), 2.36 (s, 3H), 2.30 (s, 3H), 1.01 (s, 3H).

Elemental analysis (%) calcd. For $[C_{19}H_{22}N_3PdS]^+[BAr_4]^-$: C, 47.33; H, 2.65; N, 3.25. Found: C, 47.95; H, 2.68; N, 3.22. Positive ion ESI-MS: m/z (%) = 430.0567 (100 %) $[M]^+$. Negative ion ESI-MS: m/z (%) 863.0646 (100 %) $[M]^-$.

Synthesis of $k^3-N_{pz}^{\wedge}N_{py}^{\wedge}Se-2-((3,5\text{-di-tert-butyl-1H-pyrazol-1-yl)methyl)-6-(phenylselanylmethyl)pyridinemethylpalladium(II) tetrakis(3,5-trifluoromethylphenyl)borate (3b)$.

Complex **3b** was synthesised from complex **3a** (100 mg, 0.168 mmol) and $NaBAr_4$ (148.4 mg, 0.168 mmol) according to the procedure used for the synthesis of complex **1b**. Yield: 213 mg (~89%). 1H NMR (400 MHz, $CDCl_3$, δ ppm): 7.68-7.62 (m, 10 H), 7.49 (s, 5H), 7.40 (t, 1H, $J = 7.2$ Hz), 7.34-7.27 (m, 3H), 7.12 (d, 1H, $J = 7.6$ Hz), 6.14 (s, 1H), 5.79-5.67 (m, 2H), 4.62 (d, 1H, $J = 16.0$ Hz), 4.34 (bs, 1H), 1.55 (s, 9H), 1.42 (s, 9H), 1.03 (s, 3H). Elemental analysis (%) calcd. For $[C_{25}H_{34}N_3PdSe]^+[BAr_4]^-$: C, 48.04; H, 3.25; N, 2.95. Found: C, 47.22; H, 3.22; N, 2.90. Positive ion ESI-MS: m/z (%) = 562.0973 (15%) $[M]^+$. Negative ion ESI-MS: m/z (%) 863.0653 (100%) $[M]^-$.

Synthesis of $k^3-N_{pz}^{\wedge}N_{py}^{\wedge}S-2-((3,5\text{-dimethyl-1H-pyrazol-1-yl)methyl)-6-(phenylselanylmethyl)pyridinemethylpalladium(II) tetrakis(3,5-trifluoromethylphenyl)borate (4b)$.

Complex **4b** was synthesised from complex **4a** (100 mg, 0.195 mmol) and $NaBAr_4$ (172.7 mg, 0.195 mmol) according to the procedure used for the synthesis of complex **1b**. Yield: 211 mg (~81%). 1H NMR (400 MHz, $CDCl_3$, δ ppm): 7.71-7.67 (m, 10 H), 7.52 (t, 1H, $J = 7.6$

Hz), 7.46 (s, 4H), 7.42 (t, 1H, J = 7.2 Hz), 7.34 (t, 2H, J = 7.6 Hz), 7.21-7.16 (m, 2H), 6.00 (s, 1H), 5.36-5.20 (m, 2H), 4.64 (d, 1H, J = 14.4 Hz), 4.34 (d, 1H, J = 15.6 Hz), 2.36 (s, 3H), 2.29 (s, 3H), 1.00 (s, 3H). Elemental analysis (%) calcd. For $[\text{C}_{19}\text{H}_{22}\text{N}_3\text{PdSe}]^+ [\text{BAr}_4]^-$: C, 45.68; H, 2.56; N, 3.13. Found: C, 46.21; H, 2.53; N, 3.14. Positive ion ESI-MS: m/z (%) = 478.0020 (100%) $[\text{M}]^+$. Negative ion ESI-MS: m/z (%) 863.0657 (100%) $[\text{M}]^-$.

Synthesis of $k^2\text{-N}_{\text{py}}\text{N}_{\text{pz}}\text{-2-}((3,5\text{-dimethyl-1H-pyrazol-1-yl)methyl)\text{-6-}(\text{phoxymethyl})\text{pyridineacetonitrilemethylpalladium(II) tetrakis}(3,5\text{-trifluoromethylphenyl})\text{borate (5b)}$.

A solution of complex **5a** (100 mg, 0.222 mmol) in dry dichloromethane (10 mL) was added to the solution of NaBAr_4 (196.8 mg, 0.222 mmol) in dry acetonitrile (15 mL) under argon. The reaction mixture was stirred further for 4 h at room temperature resulting light yellow solution. The reaction mixture was filtered through a small pad of Celite and removal of solvent in *vacuo* afforded foaming light yellow solid. Yield: 243 mg (~83%). ^1H NMR (400 MHz, CDCl_3 , δ ppm): 7.74 (t, 1H, J = 7.6 Hz), 7.67 (s, 8H), 7.62 (d, 1H, J = 8.0 Hz), 7.49 (s, 4H), 7.33 (t, 2H, J = 8.0 Hz), 7.25 (d, 1H, J = 7.6 Hz), 7.04 (t, 1H, J = 7.6 Hz), 6.97 (d, 2H, J = 8.0 Hz), 6.11 (d, 1H, J = 15.2 Hz), 5.90 (s, 1H), 5.36 (d, 1H, J = 12.0 Hz), 5.18 (d, 1H, J = 12.0 Hz), 5.11 (d, 1H, J = 15.2 Hz), 2.50 (d, 6H, J = 2.8 Hz), 1.85 (s, 3H), 1.04 (s, 3H). Elemental analysis (%) calcd. For $[\text{C}_{21}\text{H}_{25}\text{N}_4\text{PdO}]^+ [\text{BAr}_4]^-$: C, 48.26; H, 2.83; N, 4.25. Found; C, 48.11; H, 2.86; N, 4.01. Positive ion ESI-MS: m/z (%) = 414.0794 (15%) $[\text{M-CH}_3\text{CN}]^+$. Negative ion ESI-MS: m/z (%) 863.0651 (100%) $[\text{M}]^-$.

General procedure for CO insertion reaction in the complexes 1b-4b.

In a typical procedure, a solution of respective complex (~7 mg) in CDCl₃ (0.6 mL) in a J. Young NMR tube was carefully evacuated and then brought under ~2 atm CO pressure two to three times. Afterwards, progress of reaction was monitored by ¹H NMR spectroscopy at room temperature. All reactions were completed within 1-2 h.

***k*³-N_{pz}[^]N_{py}[^]S-2-((3,5-di-tert-butyl-1H-pyrazol-1-yl)methyl)-6-(phenylthiomethyl)pyridine acylpalladium(II) tetrakis(3,5-trifluoromethylphenyl)borate (1c).** IR (solution, cm⁻¹): 1713 ν(C=O). ¹H NMR (400 MHz, CDCl₃, δ ppm): 7.67 (s, 8H), 7.54 (t, 2H, J = 8.0 Hz), 7.50 (d, 1H, J = 8.0 Hz), 7.47 (s, 4H), 7.43 (d, 1H, J = 8.0 Hz), 7.39-7.33 (m, 3H), 7.08 (d, 1H, J = 8.0 Hz), 6.12 (s, 1H), 5.78 (s, 2H), 4.45 (bs, 2H), 2.59 (s, 3H, PdCOCH₃), 1.50 (s, 9H), 1.40 (s, 9H).

***k*³-N_{pz}[^]N_{py}[^]S-2-((3,5-dimethyl-1H-pyrazol-1-yl)methyl)-6-(phenylthiomethyl)pyridine acylpalladium(II) tetrakis(3,5-trifluoromethylphenyl)borate (2c).** IR (solution, cm⁻¹): 1711 ν(C=O). ¹H NMR (400 MHz, CDCl₃, δ ppm): 7.67 (s, 8H), 7.63 (d, 2H, J = 8.0 Hz), 7.50 (t, 1H, J = 8.0 Hz), 7.46 (s, 4H), 7.44 (d, 1H, J = 8.0 Hz), 7.39 (t, 2H, J = 8.0 Hz), 7.17 (d, 2H, J = 8.0 Hz), 6.02 (s, 1H), 5.28 (s, 2H), 4.53 (bs, 2H), 2.55 (s, 3H, PdCOCH₃), 2.28 (s, 3H), 2.18 (s, 3H).

***k*³-N_{pz}[^]N_{py}[^]Se-2-((3,5-di-tert-butyl-1H-pyrazol-1-yl)methyl)-6-(phenylselanylmethyl)pyridine acylpalladium(II) tetrakis(3,5-trifluoromethylphenyl)borate (3c).** IR (solution, cm⁻¹): 1710 ν(C=O). ¹H NMR (400 MHz, CDCl₃, δ ppm): 7.67 (s, 8H), 7.60

(d, 2H, J = 8.0 Hz), 7.50 (t, 1H, J = 8.0 Hz), 7.47 (s, 4H), 7.40 (t, 1H, J = 7.2 Hz), 7.32 (t, 3H, J = 8.0 Hz), 7.07 (d, 1H, J = 8.0 Hz), 6.11 (s, 1H), 5.84 (bs, 2H), 4.55 (bs, 1H), 4.29 (bs, 1H), 2.60 (s, 3H, PdCOCH₃), 1.50 (s, 9H), 1.39 (s, 9H).

***k*³-N_{pz}[^]N_{py}[^]Se-2-((3,5-dimethyl-1H-pyrazol-1-yl)methyl)-6-(phenylselanylmethyl)pyridine acylpalladium(II) tetrakis(3,5-trifluoromethylphenyl)borate (4c).** IR (solution, cm⁻¹): 1711 ν(C=O). ¹H NMR (400 MHz, CDCl₃, δ ppm): 7.70-7.68 (m, 10 H), 7.48 (t, 1H, J = 7.6 Hz), 7.47 (s, 4H), 7.41 (t, 1H, J = 7.6 Hz), 7.35 (t, 2H, J = 7.6 Hz), 7.16 (t, 2H, J = 7.6 Hz), 6.01 (s, 1H), 5.32 (s, 2H), 4.50 (s, 2H), 2.55 (s, 3H, PdCOCH₃), 2.27 (s, 3H), 2.20 (s, 3H).

Carbon monoxide insertion reaction in 5b.

This reaction was carried out at -50 °C and also ¹H NMR spectrum was recorded at the same temperature. The CDCl₃ solution of complex **5b** was degassed in J. Young NMR tube and CO gas was filled carefully while keeping the solution in NMR tube frozen using liq. N₂. Now progress of reaction was monitored by ¹H NMR spectroscopy at -50 °C and this reaction was completed in 1 h.

***k*²-N_{py}[^]N_{pz}[^]-2-((3,5-dimethyl-1H-pyrazol-1-yl)methyl)-6-(phenoxy)methyl)pyridine acylcarbonylpalladium(II) tetrakis(3,5-trifluoromethylphenyl)borate (5c).** ¹H NMR (400 MHz, CDCl₃, δ ppm): 7.69-7.66 (m, 9H), 7.46-7.43 (m, 5H), 7.37 (t, 2H, J = 8.0 Hz), 7.26 (d, 1H, J = 7.5 Hz), 7.08 (t, 1H, J = 7.5 Hz), 7.02 (d, 2H, J = 8.0 Hz), 5.90 (d, 1H, J = 15.5 Hz), 5.81 (s,

1H), 5.23 (d, 1H, J = 15.5 Hz), 5.14 (d, 1H, J = 12.5 Hz), 5.05 (d, 1H, J = 12.5 Hz), 2.48 (s, 3H, PdCOCH₃), 2.16 (s, 3H), 2.04 (s, 3H).

General Procedure for CO and ethylene copolymerization

In a stainless steel autoclave (50 mL) containing the catalyst precursor (0.01 mmol) and stirrer was transferred dry dichloromethane (5 mL) under an argon atmosphere. An equimolar amount of NaBAr₄ and a mixture of solvents, dichloromethane and acetonitrile (1:1, v/v) were used in the case of reactions where neutral complexes were used as catalyst precursor. The reactor was then charged with CO and ethylene. The reactor was placed on Eyela Process Station and reaction mixture was stirred at different temperatures, pressures and time. The temperature of reaction was maintained by circulating cold water through Eyela Process Station using a circulator. After completion of reaction, the autoclave was cooled under running tap water, the gas was vented, and the grey solid crude product was isolated by filtration. The solid material was purified by washing with 5 M HCl followed by water and methanol. This resulted white solid polyketone which were insoluble in common organic solvents.

Acknowledgements

Financial support for this project from the National Research Foundation (NRF), South Africa, the DST-NRF Centre of Excellence in Catalysis (c*change), South Africa and the University of Johannesburg is gratefully acknowledged. K. K. thanks University of Johannesburg for a postdoctoral fellowship.

Electronic supplementary information (ESI) available.

^1H NMR spectrum of **L1** (Fig. S1), ^1H NMR spectrum of **1a** (Fig. S2), ^1H NMR, $^{13}\text{C}\{^1\text{H}\}$ NMR and FT-IR spectra of CO/ethylene copolymer (Fig. S3-S5), DSC and TGA thermograms of CO/ethylene copolymer (Fig. S6 and S7), ^1H NMR spectra of **5b** and **5c** (Fig. S8), ^1H NMR of **5c** at variable temperature (Fig. S9), FT-IR spectrum of **1c** (Fig. S10). Crystallographic data for structural analysis (in CIF format). CCDC 1428943-1428948.

References

1. A. Nakamura, S. Ito and K. Nozaki, *Chem. Rev.*, 2009, **109**, 5215-5244.
2. S. D. Ittel, L. K. Johnson and M. Brookhart, *Chem. Rev.*, 2000, **100**, 1169–1203.
3. E. Drent and P. H. M. Budzelaar, *Chem. Rev.*, 1996, **96**, 663-681.
4. C. Bianchini and A. Meli, *Coord. Chem. Rev.*, 2002, **225**, 35-66.
5. J. Durand and B. Milani, *Coord. Chem. Rev.*, 2006, **250**, 542-560.
6. A. Nakamura, T. M. J. Anselment, J. Claverie, B. Goodall, R. F. Jordan, S. Mecking, B. Rieger, A. Sen, P. W. N. M. van Leeuwen and K. Nozaki, *Acc. Chem. Res.*, 2013, **46**, 1438-1449.
7. E. J. G. Suárez, C. Godard, A. Ruiz and C. Claver, *Eur. J. Inorg. Chem.*, **2007**, 2582-2593.
8. A. Sommazzi and F. Garbassi, *Prog. Polym. Sci.*, 1997, **22**, 1547-1605.
9. A. S. Abu-Surrah, R. Wursche and B. Rieger, *Macromol. Chem. Phys.*, 1997, **198**, 1197-1208.
10. J. Yang and H. W. Gibson, *Macromolecules*, 1997, **30**, 5629-5633.
11. H. W. Gibson and D. L. Dotson, *Polymer*, 1998, **39**, 6483-6487.
12. J. Yang and H. W. Gibson, *Macromolecules*, 1999, **32**, 8740-8746.

13. N. Yonezawa and A. Okamoto, *Polym. J.*, 2009, **41**, 899-928.
14. S. Ito, W. Wang, K. Nishimura and K. Nozaki, *Macromolecules*, 2015, **48**, 1959-1962.
15. E. Drent, J. A. M. Vanbroekhoven and M. J. Doyle, *J. Organomet. Chem.*, 1991, **417**, 235-251.
16. Z. Jiang and A. Sen, *J. Am. Chem. Soc.*, 1995, **117**, 4455-4467.
17. G. Verspui, F. Schanssema and R. A. Sheldon, *Angew. Chem. Int. Ed.*, 2000, **39**, 804-806.
18. C. Bianchini, H. M. Lee, A. Meli, W. Oberhauser, F. Vizza, P. Bruggeller, R. Haid and C. Langes, *Chem. Commun.*, 2000, 777-778.
19. J. Schwarz, E. Herdtweck and W. A. Herrmann, *Organometallics*, 2000, **19**, 3154-3160.
20. S. Doherty, G. R. Eastham, R. P. Tooze, T. H. Scanlan, D. Williams, M. R. J. Elsegood and W. Clegg, *Organometallics*, 1999, **18**, 3558-3560.
21. S. J. Dossett, A. Gillon, A. G. Orpen, J. S. Fleming, P. G. Pringle, D. F. Wass and M. D. Jones, *Chem. Commun.*, 2001, 699-700.
22. C. Bianchini, A. Meli, W. Oberhauser, S. Parisel, E. Passaglia, F. Ciardelli, O. V. Gusev, A. M. Kal'si and N. V. Vologdin, *Organometallics*, 2005, **24**, 1018-1030.
23. P. Braunstein, C. Frison and X. Morise, *Angew. Chem. Int. Ed.*, 2000, **39**, 2867-2870.
24. J. Andrieu, P. Braunstein, F. Naud and R. D. Adams, *J. Organomet. Chem.*, 2000, **601**, 43-50.
25. G. J. P. Britovsek, W. Keim, S. Mecking, D. Sainz and T. Wagner, *J. Chem. Soc., Chem. Commun.*, 1993, 1632-1634.
26. P. Braunstein, M. D. Fryzuk, M. Le Dall, F. Naud, S. J. Rettig and F. Speiser, *J. Chem. Soc., Dalton Trans.*, 2000, 1067-1074.
27. P. H. P. Brinkmann and G. A. Luinstra, *J. Organomet. Chem.*, 1999, **572**, 193-205.

28. K. R. Reddy, C.-L. Chen, Y.-H. Liu, S.-M. Peng, J.-T. Chen and S.-T. Liu, *Organometallics*, 1999, **18**, 2574-2576.
29. A. Aeby and G. Consiglio, *J. Chem. Soc., Dalton Trans.*, 1999, 655-656.
30. M. Brookhart, F. C. Rix, J. M. DeSimone and J. C. Barborak, *J. Am. Chem. Soc.*, 1992, **114**, 5894-5895.
31. B. Milani, E. Alessio, G. Mestroni, E. Zangrando, L. Randaccio and G. Consiglio, *J. Chem. Soc., Dalton Trans.*, 1996, 1021-1029.
32. C. S. Shultz, J. Ledford, J. M. DeSimone and M. Brookhart, *J. Am. Chem. Soc.*, 2000, **122**, 6351-6356.
33. W. P. Mul, E. Drent, P. J. Jansens, A. H. Kramer and M. H. W. Sonnemans, *J. Am. Chem. Soc.*, 2001, **123**, 5350-5351.
34. T. M. J. Anselment, S. I. Vagin and B. Rieger, *Dalton Trans.*, 2008, **34**, 4537-4672.
35. C. Bianchini, A. Meli, W. Oberhauser, C. Claver and E. J. G. Suarez, *Eur. J. Inorg. Chem.*, 2007, 2702-2710.
36. G. K. Barlow, J. D. Boyle, N. A. Cooley, T. Ghaffar and D. F. Wass, *Organometallics*, 2000, **19**, 1470-1476.
37. M. Svensson, T. Matsubara and K. Morokuma, *Organometallics*, 1996, **15**, 5568-5576.
38. P. Margl and T. Ziegler, *Organometallics*, 1996, **15**, 5519-5523.
39. F. C. Rix, M. Brookhart and P. S. White, *J. Am. Chem. Soc.*, 1996, **118**, 4746-4764.
40. G. P. C. M. Dekker, C. J. Elsevier, K. Vrieze, P. W. N. M. v. Leeuwen and C. F. Roobeek, *J. Organomet. Chem.*, 1992, **430**, 357-372.
41. G. P. C. M. Dekker, A. Buijs, C. J. Elsevier, K. Vrieze, P. W. N. M. v. Leeuwen, W. J. J. Smeets, A. L. Spek, Y. F. Wang and C. H. Stam, *Organometallics*, 1992, **11**, 1937-1948.

42. C. Pisano, G. Consiglio, A. Sironib and M. Moret, *J. Chem. Soc., Chem. Commun.*, 1991, 421-423.
43. P. H. M. Budzelaar, P. W. N. M. v. Leeuwen, C. F. Roobeek and A. G. Orpen, *Organometallics*, 1992, **11**, 23-25.
44. M. Sperrle, V. Gramlich and G. Consiglio, *Organometallics*, 1996, **15**, 5196-5201.
45. M. Portnoy and D. Milstein, *Organometallics*, 1994, **13**, 600-609.
46. R. E. Rulke, V. E. Kaasjager, D. Kliphuis, C. J. Elsevier, P. W. N. M. v. Leeuwen, K. Vrieze and K. Goubitz, *Organometallics*, 1996, **15**, 668-677.
47. C. Obuah, M. K. Ainooson, S. Boltina, I. A. Guzei, K. Nozaki and J. Darkwa, *Organometallics*, 2013, **32**, 980-988.
48. K. Kumar and B. D. Gupta, *J. Organomet. Chem.*, 2011, **696**, 3343-3350.
49. O. Prakash, K. N. Sharma, H. Joshi, P. L. Gupta and A. K. Singh, *Organometallics*, 2014, **33**, 983-993.
50. K. R. Reddy, K. Surekha, G.-H. Lee, S.-M. Peng, J.-T. Chen and S.-T. Liu, *Organometallics*, 2001, **20**, 1292-1299.
51. B. Milani, E. Alessio, G. Mestroni, A. Sommazzi, F. Garbassi, E. Zangrando, N. Bresciani-Pahor and L. Randaccio, *J. Chem. Soc., Dalton Trans.*, 1994, **13**, 1903-1911.
52. R. E. Rulke, D. Kliphuis, C. J. Elsevier, J. Fraanje, K. Goubitz, P. W. N. M. v. Leeuwen and K. Vrieze, *J. Chem. Soc., Chem. Commun.*, 1994, 1817-1819.
53. R. V. Asselt, E. E. C. G. Gielens, R. E. Rulke and C. J. Elsevier, *J. Chem. Soc., Chem. Commun.*, 1993, 1203-1205.
54. R. V. Asselt, E. E. C. G. Gielens, R. E. Rulke, K. Vrieze and C. J. Elsevier, *J. Am. Chem. Soc.*, 1994, **116**, 977-985.

55. S. O. Ojwach, 2008, *Nitrogen-donor nickel and palladium complexes as olefin transformation catalysts (PhD thesis, University of Johannesburg, South Africa)*.
56. H. Su, C. Wu, J. Zhu, T. Miao, D. Wang, C. Xia, X. Zhao, Q. Gong, B. Song and H. Ai, *Dalton Trans.*, 2012, **41**, 14480-14483.
57. J. Elguero, E. Gonzalez and R. Jacquier, *Bull. Soc. Chim. Fr.*, 1968, 707-713.
58. R. E. Rulke, J. M. Ernsting, A. L. Spelt, C. J. Elsevier, R. W. N. M. v. Leeuwen and K. Vrieze, *Inorg. Chem.*, 1993, **32**, 5769-5778.
59. A. A. Watson, D. A. House and P. J. Steel, *Inorg. Chim. Acta*, 1987, **130**, 167-176.
60. Bruker-AXS, SADABS, and SAINT Software Reference Manuals, Bruker-AXS, Madison, and U. Wisconsin, 2009.
61. G. M. Sheldrick and A. C. SHELXL, Sect. A: Fundam. Crystallogr., 2008, **64**, 112-122.

